Prepared for submission to JHEP

the

QCD Sum Rule s for Parameters of B-meson Distribution Amplitudes

Muslem Rahimi, Marcel Wald

Theoretische Physik 1, Naturwissenschaftlich-Technische Fakultät, Universität Siegen, D-57068 Siegen, Germany

E-mail: muslem.rahimi@uni-siegen.de, marcel.wald@uni-siegen.de

diagonal correlation function

two-point QCD

Abstract: We derive ~~alternative~~ ~~positive definite~~ sum rules for the ~~B-meson light-cone distribution amplitude parameters $\lambda^2_{E,H}$ and their ratio λ_E^2/λ_H^2 in the framework of heavy-quark effective theory~~. In this analysis, we include all ~~leading~~ contributions in the operator product expansion up to mass dimension seven.

(abtract too short, the main results should be added in a few lines)

Keywords: B Physics, Heavy Quark Physics, Nonperturbative Effects

we obtain new estimates of the parameters. … and … serving as normalization for the quark-antiquark-gluon B meson DAs defined in HQET. For that …

Contents

1 Introduction

Comment on the order: first definition, then factorization and other uses, after that the parameters and finally use of sum rules

Light-cone distribution amplitudes (LCDAs) are important ingredients for B-meson factorization theorems. This factorization approach has originally been designed for charmless non-leptonic B-meson decays like $B \to \pi\pi$ or $B \to \pi K$ in the heavy quark limit [1–3] and allows for the study of CP-violation in weak interactions. The B-meson distribution amplitude s encode~~s~~ the non-perturbative nature of the interaction in these decays, ~~since~~ T they parameterize non-local heavy-light ~~currents~~ quark operators at leading order in the heavy-quark effective theory (HQET) [4] ~~in terms of~~ expansions in wave functions of increasing twist. But contrary to the light-meson distribution amplitudes which also appear in the factorization theorems, there is not much known about B-meson distribution amplitudes. General ~~expressions~~ definitions for the B-meson LCDAs have been ~~obtained~~ given in [~~5, 6~~]. ~~Due to their~~ factorization scale dependence, the evolution equations have been investigated for the leading twist two-particle LCDA in [7–11] and for higher twist amplitudes in [12]. In order to derive general properties of the B-meson LCDAs, the decay $B \to \gamma\ell\nu$ is of particular interest. At large photon energies of the order of m_b, factorization is a very useful tool to study for example the form factors or the inverse moment λ_B [13–18]. Beyond the leading order in α_s, LCDAs have been investigated e.g. in [6, 19] and first and second moments of the LCDAs have been defined within these works. There, three-particle LCDAs are parameterized by the parameters $\lambda_{E,H}^2$, which contribute to the second moments in the $\mathcal{O}(\alpha_s)$ expansion of the distribution amplitudes. Estimates for these parameters have been obtained using QCD sum rules embedded into the HQET framework [20] and similar work has already been done in the case of π- or K-mesons [21].

strong

?

[3,19]

?

?

?

The parameters are of particular interest in this work and have been first investigated by Grozin and Neubert [19].

repetition

In their work, Grozin and Neubert [19] obtained estimates by considering all contributions up to mass dimension five. For this, they investigated all leading order contributions to the sum rules. Up to dimension four, the leading order contribution starts at $\mathcal{O}(\alpha_s)$, while the leading order of mass dimension five starts at $\mathcal{O}(\alpha_s^0)$. They obtained the following values:

$$\begin{aligned} \lambda_H^2(\mu) &= (0.18 \pm 0.07)\ \mathrm{GeV}^2\,, \\ \lambda_E^2(\mu) &= (0.11 \pm 0.06)\ \mathrm{GeV}^2. \end{aligned} \tag{1.1}$$

at $\mu = 1$ GeV. The extraction of these estimates is connected with a rather large uncertainty, because the sum rules turn out to be unstable with respect to the variation of the Borel parameter. Notice that such a dependence is not unexpected, since it is well known [22, 23] that higher dimensional condensates tend to give large contributions to correlation functions including higher dimensional operators.

Further studi~~es~~ y by Nishikawa and Tanaka [24] lead to deviations from the original values for $\lambda_{E,H}^2$. These authors argued in their work that a consistent treatment of all

$\mathcal{O}(\alpha_s)$ contributions should resolve the stability problem, which is related to the fact that the operator-product expansion (OPE) does not converge for the parameters $\lambda^2_{E,H}$ in [19]. For this analysis, they included the $\mathcal{O}(\alpha_s)$ corrections of the coupling constant $F(\mu)$ as well, which, albeit leading to good convergence of the OPE, obey large higher order perturbative corrections [25, 26]. Moreover, they included as an additional non-perturbative correction the dimension six diagram of $\mathcal{O}(\alpha_s)$ in

? order to check whether the OPE starts to converge beyond mass dimension five and calculated the $\mathcal{O}(\alpha_s)$ corrections for the dimension five condensate. After performing a resummation of the large logarithmic contributions, which results into more stable sum rules and into a more convergent OPE compared to [19], the following values have been obtained:

$$\begin{aligned} \lambda^2_H(1\ \text{GeV}) &= (0.06 \pm 0.03)\ \text{GeV}^2\,, \\ \lambda^2_E(1\ \text{GeV}) &= (0.03 \pm 0.02)\ \text{GeV}^2\,. \end{aligned} \tag{1.2}$$

see Table

Their estimates differ by approximately a factor of three from Eq. (1.1), although the ratio λ^2_E/λ^2_H gives nearly the same value.

? In order to resolve this tension, we ~~are going to~~ investigate an alternative sum rule, which also allows for predictions of $\lambda^2_{E,H}$. Instead of analysing a correlation function with a three-particle and a two-particle current, we consider the ~~diagonal~~ new sum rule based in diag. corr. function of ~~between~~ two quark-antiquark-gluon three-particle currents. We include all ~~non-vanishing~~ leading order contributions up to ~~corrections of~~ mass dimension seven. The hence, duality. advantage of this sum rule is that it is positive definite. OPE is not better than for nondiagonal case But due to the high mass dimension of the correlation function, we expect that continuum and higher excited states are dominating the sum rule. Moreover, This problem will be resolved by considering combinations of the parameters $\lambda^2_{E,H}$.

The paper is organised as follows: In Section 2 we derive the sum rules for the parameters $\lambda^2_{E,H}$ and the sum $(\lambda^2_H + \lambda^2_E)$. Section 3 is devoted to the computation of OPE the contributions which enter the sum rules. In Section 4 we discuss the numerical analysis of the sum rules and present our final results for the parameters $\lambda^2_{E,H}$. Additionally, we investigate the ratio given by the quotient of these parameters. Finally, we conclude in Section 5.

2 Derivation of the QCD Sum Rules in HQET

In this chapter we ~~are going to~~ derive the sum rules for the diagonal quark-antiquark-gluon three-particle correlation function. Before we start, the definition of the HQET parameter $\lambda^2_{E,H}$ is in order [19]:

$$\begin{aligned} \langle 0|\, g_s \bar{q}\, \vec{\alpha}\cdot\vec{E}\, \gamma_5 h_v\, |\bar{B}(v)\rangle &= F(\mu)\, \lambda_E^2\,, \\ \langle 0|\, g_s \bar{q}\, \vec{\sigma}\cdot\vec{H}\, \gamma_5 h_v\, |\bar{B}(v)\rangle &= iF(\mu)\, \lambda_H^2. \end{aligned} \tag{2.1}$$

From a physical point of view, these quantities parameterize the vacuum to $\bar{B}$-meson matrix elements of the chromoelectric and chromomagnetic fields in HQET. The chromoelectric field is $E^i = G^{0i}$ and $H^i = -\frac{1}{2}\epsilon^{ijk}G^{jk}$ denotes the chromomagnetic field, with $G_{\mu\nu} = G^a_{\mu\nu}T^a$. Here, the tensor $G^{\mu\nu} = \frac{i}{g_s}[D^\mu, D^\nu]$ is ~~defined to be~~ the field strength tensor, while g_s corresponds to the strong coupling constant. Furthermore, the fields $\bar{q}$ in Eq. (2.1) indicate light quark fields, whereas the field h_v denotes the HQET heavy quark field. Moreover, v is the velocity of the heavy $\bar{B}$-meson. The Dirac matrices α^i is given by $\gamma^0\gamma^i$ and $\sigma^i = \gamma^i\gamma^5$. In addition to that, the HQET decay constant $F(\mu)$ is defined via the matrix element ??

$$\langle 0|\, \bar{q}\gamma_\mu\gamma_5 h_v\, |\bar{B}(v)\rangle = iF(\mu)v_\mu \tag{2.2}$$

and can be related to the $\bar{B}$-meson decay constant in QCD up to one loop order [27]:

$$f_B\sqrt{m_B} = F(\mu)K(\mu) = F(\mu)\Big[1 + \frac{C_F\alpha_s}{4\pi}\Big(3\cdot\ln\frac{m_b}{\mu} - 2\Big) + ...\Big] + \mathcal{O}\Big(\frac{1}{m_b}\Big). \tag{2.3}$$

Its explicit scale dependence has to cancel with the one of the matching prefactor in order to lead to the constant f_B. Values for f_B can be found in [28] and estimate this decay constant to be:

$$f_B = (192.0 \pm 4.3)\ \text{MeV}\,. \tag{2.4}$$

The coupling constant $F(\mu)$ will be of particular importance in the derivation of the relevant low-energy parameters.

As already discussed before, Grozin and Neubert [19] introduced the parameters $\lambda^2_{E,H}$. For this, they considered the correlation function:

$$\Pi_{\mathrm{GN}} = i\int \mathrm{d}^d x e^{-i\omega v\cdot x}\, \langle 0|\, T\{\bar{q}(0) g_s \Gamma_1^{\mu\nu} G_{\mu\nu}(0) h_v(0)\bar{h}_v(x)\gamma_5 q(x)\}\, |0\rangle\ . \tag{2.5}$$

The starting point for our calculation is the correlation function:

$$\Pi_{\mathrm{diag}} = i\int \mathrm{d}^d x\; e^{-i\omega v\cdot x}\, \langle 0|\, T\{\bar{q}(0)\Gamma_1^{\mu\nu} g_s G_{\mu\nu}(0) h_v(0)\bar{h}_v(x)\Gamma_2^{\rho\sigma} g_s G_{\rho\sigma}(x) q(x)\}\, |0\rangle \tag{2.6}$$

Notice that at this point we do not require a specific choice of the quantities $\Gamma_1^{\mu\nu}$ and $\Gamma_2^{\rho\sigma}$, which indicate an arbitrary combination of Dirac γ-matrices, but in the following steps it is convenient to choose these matrices such that combinations of the HQET parameters $\lambda_{E,H}^2$ are projected out. This requires that the perturbative and non-perturbative contributions to the spectral density in Section 3 are computed for general $\Gamma_1^{\mu\nu}$ and $\Gamma_2^{\rho\sigma}$. Since we are considering a diagonal Greens function, the structure of $\Gamma_2^{\rho\sigma}$ is directly related to $\Gamma_1^{\mu\nu}$ by replacing indices. From now on we use the notation:

$$\Gamma_1 \equiv \Gamma_1^{\mu\nu}\,, \tag{2.7}$$?

$$\Gamma_2 \equiv \Gamma_2^{\mu\nu}\,. \tag{2.8}$$

Moreover, we are working in the B-meson rest frame, where $v = (1, \vec{0})^T$, in order to simplify the calculations.

The next step in the derivation of the sum rules will be to exploit the unitary condition, where the ground state B-meson is separated from the continuum and excited states:

$$\begin{aligned}
\frac{1}{\pi}\mathrm{Im}\Pi_{\text{diag}}(\omega) = & \sum_n (2\pi)^3\delta(\omega - p_n)\,\langle 0|\,\bar{q}(0)\Gamma_1 g_s G_{\mu\nu}(0)h_v(0)\,|n\rangle\,\langle n|\,\bar{h}_v(x)\Gamma_2 g_s G_{\rho\sigma}(x)q(x)\,|0\rangle\,\mathrm{d}\Phi_n \\
= & \;\delta(\omega - \bar{\Lambda})\Theta(\omega^0)\,\langle 0|\,\bar{q}(0)\Gamma_1 g_s G_{\mu\nu}(0)h_v(0)\,|B\rangle\,\langle B|\,\bar{h}_v(x)\Gamma_2 g_s G_{\rho\sigma}(x)q(x)\,|0\rangle \\
& + \rho^{\text{hadr.}}(\omega)\Theta(\omega - s^{th})
\end{aligned} \tag{2.9}$$

In Eq. (2.9), we introduced the binding energy $\bar{\Lambda} = m_B - m_b$, which is one of the important low-energy parameters in this formalism. Furthermore, we separated the
? full n-particle phase space in the first line into a ground state contribution, which will be the dominant contribution in our chosen stability window, and a continuum contribution including broad higher resonances. In the case of QCD correlation functions, the exponential in Eq. (2.6) would generally take the form e^{-iqx} with q denoting the external momentum. Due to the fact that there is no spatial component in the B-meson rest frame, transitions from the ground state to the excited states in Eq. (2.9) are possible by injecting energy q^0 into the system. In this work we explicitly chose $q = \omega \cdot v$ such that we end up with the correlation function shown in Eq. (2.6).

The matrix elements occurring in (2.9) can be decomposed in the following way [19, 24]:

$$\begin{aligned}
\langle 0|\,\bar{q}(0)\Gamma_1 g_s G_{\mu\nu}(0)h_v(0)\,|B\rangle = & \frac{-i}{6}F(\mu)\{\lambda_H^2(\mu)\cdot\mathrm{Tr}[\Gamma_1 P_+\gamma_5\sigma_{\mu\nu}] \\
& + [\lambda_H^2(\mu) - \lambda_E^2(\mu)]\cdot\mathrm{Tr}[\Gamma_1 P_+\gamma_5(iv_\mu\gamma_\nu - iv_\nu\gamma_\mu)]\}.
\end{aligned} \tag{2.10}$$

Notice that the second decomposition is indeed valid since the B-meson ground state explicitly depends on the velocity v and $\sigma_{\mu\nu} = \frac{i}{2}[\gamma_\mu, \gamma_\nu]$ corresponds to the usual antisymmetric Dirac bilinear. In (2.10) we made use of the covariant trace formalism, further investigated in [19, 29].

The next step will be to use the standard dispersion relation, after using residue theorem and the Schwartz reflection principle [1]:

$$
\begin{aligned}
\Pi_{\text{diag}}(\omega) = &\frac{1}{\pi}\int_0^\infty \mathrm{d}s \frac{\mathrm{Im}\Pi_{\text{diag}}(\omega)}{s-\omega-i0^+} \\
=&\frac{1}{\bar{\Lambda}-\omega-i0^+}\langle 0|\,\bar{q}(0)\Gamma_1 g_s G_{\mu\nu}(0)h_v(0)\,|B\rangle\,\langle B|\,\bar{h}_v(x)\Gamma_2 g_s G_{\rho\sigma}(x)q(x)\,|0\rangle \\
&+\int_{s^{th}}^\infty \mathrm{d}s\frac{\rho^{\text{hadr.}}(s)}{s-\omega-i0^+}
\end{aligned}
\tag{2.11}
$$

In Eq. (2.11) we introduce the threshold parameter s^{th}, which is a relevant low-energy parameter that separates the ground state contribution from higher resonances and continuum contributions.

We can now move on and evaluate the ground state contribution:

$$
\begin{aligned}
&\langle 0|\,\bar{q}(0)\Gamma_1 g_s G_{\mu\nu}(0)h_v(0)\,|B\rangle\,\langle B|\,\bar{h}_v(x)\Gamma_2 g_s G_{\rho\sigma}(x)q(x)\,|0\rangle \\
=&\frac{-i}{6}F(\mu)\Big[\lambda_H^2(\mu)\mathrm{Tr}[\Gamma_1 P_+\gamma_5\sigma_{\mu\nu}]+[\lambda_H^2(\mu)-\lambda_E^2(\mu)]\mathrm{Tr}[\Gamma_1 P_+\gamma_5(iv_\mu\gamma_\nu-iv_\nu\gamma_\mu)]\Big] \\
&\times\frac{-i}{6}F^\dagger(\mu)\Big[\lambda_H^2(\mu)\mathrm{Tr}[\gamma_5 P_+\Gamma_2\sigma_{\rho\sigma}]-[\lambda_H^2(\mu)-\lambda_E^2(\mu)]\mathrm{Tr}[\gamma_5 P_+\Gamma_2(iv_\rho\gamma_\sigma-iv_\sigma\gamma_\rho)]\Big]
\end{aligned}
\tag{2.12}
$$

Notice that the term involving the difference of both HQET parameter $(\lambda_H^2-\lambda_E^2)$ does not change its sign under complex conjugation.

In order to derive the sum rules which ultimately determine the parameters $\lambda_{E,H}^2$, we make an explicit choice for the matrices Γ_1 and Γ_2 [19]. Following the same approach as [24], we choose our gamma matrices $\Gamma_{1,2}$ as:

$$
\Gamma_1 = \frac{i}{2}\sigma_{\mu\nu}\gamma_5 \tag{2.13}
$$

to obtain $(\lambda_H^2+\lambda_E^2)^2$ sum rule. Furthermore, for the projection of λ_H^4 sum rule we choose:

$$
\Gamma_1 = i\left(\frac{1}{2}\delta_\alpha^{\ \nu}-v_\nu v^\alpha\right)\sigma_{\mu\alpha}\gamma_5 \tag{2.14}
$$

[1]For more details on QCD sum rules or HQET sum rules, see [30, 31]

and for λ_E^4:

$$\Gamma_1 = i v_\nu v^\alpha \sigma_{\mu\alpha}\gamma_5. \tag{2.15}$$

Notice that these choices are Lorentz covariant in comparison to Eq. (2.1). The corresponding expressions for Γ_2 can be obtained from Γ_1 by replacing $\mu \to \rho$, $\nu \to \sigma$. Using the relation in Eq. (2.12), we can obtain expressions for $\Pi_{H,E}$ and Π_{HE}:

$$\Pi_{H,E}(\omega) = F(\mu)^2 \cdot \lambda_{H,E}^4 \cdot \frac{1}{\bar{\Lambda} - \omega - i0^+} + \int_{s^{th}}^{\infty} \mathrm{d}s \frac{\rho_{H,E}^{\text{hadr.}}(s)}{s - \omega - i0^+} \tag{2.16}$$

$$\Pi_{HE}(\omega) = F(\mu)^2 \cdot (\lambda_H^2 + \lambda_E^2)^2 \cdot \frac{1}{\bar{\Lambda} - \omega - i0^+} + \int_{s^{\text{th}}}^{\infty} \mathrm{d}s \frac{\rho_{HE}^{\text{hadr.}}(s)}{s - \omega - i0^+} \tag{2.17}$$

Note that, the threshold parameter in Eq. (2.16) does not necessarily coincide with the threshold parameter in Eq. (2.17).

~~Since it is hard~~ to parameterize the hadronic spectral density, we make use of the global and semi-local quark-hadron duality (QHD) [32, 33] in order to connect the hadronic spectral density with the spectral density which is described by the OPE [27, 31, 34, 35]. This is the essential idea of this formalism. However, power suppressed non-perturbative effects become dominant in comparison to the perturbative contribution for $\cancel{-}\omega \approx \Lambda_{\text{QCD}}$. In the QCD sum rule approach ~~by~~ [35], these effects were parameterized in terms of a power series of ~~higher-dimensional~~ local condensates as a consequence of the non-trivial QCD vacuum. These condensates carry the quantum numbers of the QCD vacuum. For convenience, we show explicitly in Appendix A the expansion and averaging of the vacuum matrix element (2.6) in order to obtain the quark condensate $\langle 0|\, \bar{q}q \,|0\rangle$, the gluon condensate $\langle 0|\, G^a_{\mu\nu} G^b_{\rho\sigma} \,|0\rangle$, the quark-gluon condensate $\langle 0|\, \bar{q} g_s \sigma \cdot G q \,|0\rangle$ and the triple-gluon condensate $\langle 0|\, g_s^3 f^{abc} G^a_{\mu\nu} G^b_{\rho\sigma} G^c_{\alpha\lambda} \,|0\rangle$.

Although we can handle the Euclidean region, the physical states described by the spectral function in Eq. (2.16) and (2.17) are defined for $\omega \in \mathbb{R}$. But since there is no estimate for the hadronic spectral density $\rho_X^{\text{hadr.}}(s)$, we need to make use of two statements. First, we exploit that for $\omega \ll 0$ the hadronic and the OPE spectral functions coincide at the global level:

$$\Pi_X^{\text{hadr.}} = \Pi_X^{\text{OPE}} \quad \text{for } X \in \{H, E, HE\}. \tag{2.18}$$

Asymptotic freedom guarantees that this equality holds. Moreover, we need to employ the semi-local quark-hadron duality, which connects the spectral densities:

$$\int_{s_X^{th}}^{\infty} \mathrm{d}s \frac{\rho_X^{\text{hadr.}}(s)}{s - \omega - i0^+} = \int_{s_X^{th}}^{\infty} \mathrm{d}s \frac{\rho_X^{\text{OPE}}(s)}{s - \omega - i0^+}, \tag{2.19}$$

where X can be chosen according to (2.18). In the low-energy region, where non-perturbative effects dominate, the duality relation is largely violated due to strong resonance peaks, while in the high-energy region these peaks become broad and overlapping. Once a sum rule is obtained, the approximations made by QHD are consistent (see Section 4 for more details). So it is necessary to work in the transition region where the condensates are important, but still small and local enough such that perturbative methods can be applied.

Based on the relation in Eq. (2.18), (2.19) and separating the integral over the OPE spectral density by introducing the threshold parameter s^{th}, we end up with the final form of the sum rules:

$$F(\mu)^2 \cdot \lambda_{H,E}^4 \frac{1}{\bar{\Lambda} - \omega - i0^+} = \int_0^{s^{th}} \mathrm{d}s \frac{\rho_{H,E}^{\mathrm{OPE}}(s)}{s - \omega - i0^+}\,, \tag{2.20}$$

$$F(\mu)^2 \cdot (\lambda_H^2 + \lambda_E^2)^2 \frac{1}{\bar{\Lambda} - \omega - i0^+} = \int_0^{s^{th}} \mathrm{d}s \frac{\rho_{HE}^{\mathrm{OPE}}(s)}{s - \omega - i0^+}. \tag{2.21}$$

Finally, we perform a Borel transformation, which removes possible substraction terms and leads further to an exponential suppression of higher resonances and the continuum. In addition to that, the convergence of our sum rule is improved. Generally, the Borel transform can be defined in the following way [30, 31]:

$$\mathcal{B}_M f(\omega) = \lim_{n\to\infty, -\omega\to\infty} \frac{(-\omega)^{n+1}}{\Gamma(n+1)} \left(\frac{\mathrm{d}}{\mathrm{d}\omega}\right)^n f(\omega), \tag{2.22}$$

where $f(\omega)$ illustrates an arbitrary test function. Furthermore, we keep the ratio $M = \frac{-\omega}{n}$ fixed, M denotes the Borel parameter.
After applying this transformation, we derive the final form of our sum rule expressions:

$$F(\mu)^2 \cdot \lambda_{H,E}^4 \cdot e^{-\bar{\Lambda}/M} = \int_0^{\omega_{th}} \mathrm{d}\omega\; \rho_{H,E}^{\mathrm{OPE}}(\omega)\; e^{-\omega/M} = \int_0^{\omega_{\mathrm{th}}} \mathrm{d}\omega\; \frac{1}{\pi} \mathrm{Im}\Pi_{H,E}^{\mathrm{OPE}}(\omega)\; e^{-\omega/M} \tag{2.23}$$

$$F(\mu)^2 \cdot (\lambda_H^2 + \lambda_E^2)^2 \cdot e^{-\bar{\Lambda}/M} = \int_0^{\omega_{th}} \mathrm{d}\omega\; \rho_{HE}^{\mathrm{OPE}}(\omega)\; e^{-\omega/M} = \int_0^{\omega_{\mathrm{th}}} \mathrm{d}\omega\; \frac{1}{\pi} \mathrm{Im}\Pi_{HE}^{\mathrm{OPE}}(\omega)\; e^{-\omega/M} \tag{2.24}$$

These are the HQET sum rules presented in the paper. In order to obtain reliable sum rules, the Borel parameter M needs to be chosen accordingly together with the threshold parameter ω_{th}. The next step will be to determine the spectral function $\Pi_X^{\mathrm{OPE}}(s)$, which is given by the OPE:

$$\begin{aligned}\Pi_{\mathrm{X}}^{\mathrm{OPE}}(\omega) = {} & C_{\mathrm{pert}}^{\mathrm{X}}(\omega) + C_{\bar{q}q}^{\mathrm{X}} \langle \bar{q}q \rangle + C_{G^2}^{\mathrm{X}} \langle \frac{\alpha_s}{\pi} G^2 \rangle + C_{\bar{q}Gq}^{\mathrm{X}} \langle \bar{q} g_s \sigma \cdot G q \rangle \\ & + C_{G^3}^{\mathrm{X}} \langle g_s^3 f^{abc} G^a G^b G^c \rangle + C_{\bar{q}qG^2}^{\mathrm{X}} \langle \bar{q}q \rangle \langle \frac{\alpha_s}{\pi} G^2 \rangle + \ldots\end{aligned} \tag{2.25}$$

The Wilson coefficients C in Eq. (2.25) will be discussed in Section 3. Moreover, we define a more convenient notation for the condensate contributions:

$$\langle \bar{q}q \rangle := \langle 0| \, \bar{q}q \, |0\rangle \, , \langle G^2 \rangle := \langle 0| \, G^a_{\mu\nu} G^{a,\mu\nu} \, |0\rangle \, , \langle \bar{q} g_s \sigma \cdot G q \rangle := \langle 0| \, \bar{q} g_s G^{\mu\nu} \sigma_{\mu\nu} q \, |0\rangle \, ,$$
$$\langle g_s^3 f^{abc} G^a G^b G^c \rangle := \langle 0| \, g_s^3 f^{abc} G^a_{\mu\nu} G^{b,\nu\rho} G^{c,\mu}_{\rho} \, |0\rangle \, . \tag{2.26}$$

As previously mentioned, the condensates are uniquely parameterized up to mass dimension five. Starting at dimension six and higher, there occur many different possible contributions, but some of them are related by QCD equations of motions and Fierz identities [36] to each other [2]. Note that, in the power expansion of Eq. (2.25) we have only stated the dimension six and seven condensates, which give a leading order contribution to the parameters $\lambda^2_{E,H}$.

Moreover, there are many estimates for the values of the condensates given in the literature, which have been obtained from e.g. lattice QCD, sum rules [37], but obtaining values for condensates of dimension six and higher is an ongoing task due to the mixing with lower dimensional condensates. Because of the lack of these values, the vacuum saturation approximation [38] is exploited in many cases, where a full set of intermediate states is introduced into the higher dimensional condensate and the assumption is used that only the ground state gives a dominant contribution. Thus, the higher dimensional condensate will be effectively reduced to a combination of lower dimensional condensates [3].

[2] A list is given for example in the review [37].

[3] This has already been done for the dimension seven condensate in Eq. (2.25)

3 Computation of the Wilson Coefficients

In this chapter, the leading perturbative and non-perturbative contributions to the correlation function in (2.16) and (2.17) are calculated up to dimension seven. Since the leading order of the diagonal correlator of two three-particle currents is of order $\mathcal{O}(\alpha_s)$, we only investigate contributions up to this order in perturbation theory. For the perturbative contribution we choose the Feynman gauge for the background field, while the contributions starting at mass dimension three are evaluated in the fixed-point or Fock-Schwinger (FS) gauge [39, 40]:

$$x_\mu A^\mu(x) = 0 \qquad \text{and} \qquad A_\mu(x) = \int_0^1 \mathrm{d}u\, u x^\nu G_{\nu\mu}(ux). \tag{3.1}$$

In the FS gauge, we set the reference point to $x_0 = 0$. This reference point would occur in all intermediate steps of the calculation and cancel in the end of the calculation. It is well known that this gauge is particularly useful in QCD sum rule computations.

Within the framework of QCD sum rules, the long-distance effects are encoded in local vacuum matrix elements of increasing mass dimension. In order to obtain these local condensates, the gluon field strength tensor is expanded in x, which results into a simple relation between the gluon field A_μ and the field strength tensor $G_{\mu\nu}$. Additionally, gluon fields do not interact with the heavy quark in HQET, which can be easily seen by considering the heavy-quark propagator in position space [24]:

$$\overbrace{h_v(0)\bar{h}_v(x)} = \Theta(-v\cdot x)\,\delta^{(d-1)}(x_\perp)\,P_+\,\mathcal{P}\exp\left(ig_s\int_{v\cdot x}^{0}\mathrm{d}s v\cdot A(sv)\right). \tag{3.2}$$

Here, $x_\perp^\mu = x^\mu - (v\cdot x)v^\mu$, $P_+ = (1+\not{v})/2$ denotes the projection operator and $\mathcal{P}$ illustrates the path ordering operator. Besides these simplifications, there are three additional vanishing subdiagrams depicted in Figure 5 due to the FS gauge.

Generally, all diagrams can be evaluated in position space like in [19, 24], but in this work we choose to work in momentum space. We make use of dimensional regularization for the loop integrals with the convention $d = 4-2\epsilon$. Figure 1-5 [4] show the diagrams which need to be evaluated in order to obtain the Wilson coefficients in Eq. (2.25). The calculation of these coefficients proceeds in the following way: First, we use FeynCalc [42–44] to decompose tensor integrals to scalar integrals. In the next step, these scalar integrals are reduced to master integrals by integration-by-parts identities using LiteRed [45, 46].

We start by considering the perturbative and mass dimension three condensate in Fig. 1:

[4] All diagrams in this work have been created with JaxoDraw [41].

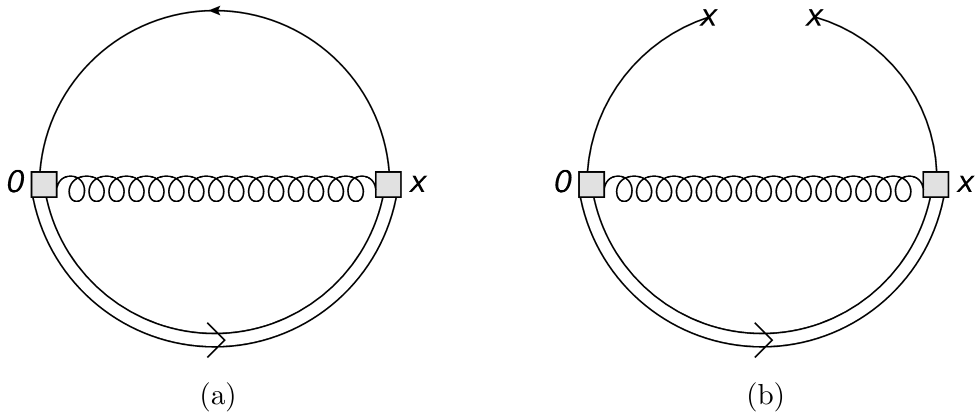

Figure 1: Feynman diagrams for the perturbative and $\langle \bar{q}q \rangle$ condensate contribution. The double line denotes the heavy quark propagator. The solid line denotes the light quark propagator and the curly line denotes the gluon propagator.

$$
\begin{aligned}
C^{\mathrm{X}}_{\mathrm{pert}}(\omega) = &\frac{2\alpha_s}{\pi^3} \cdot C_F N_c \cdot \mathrm{Tr}[\Gamma_1 P_+ \Gamma_2 \not{v}] \cdot \mu^{4\epsilon} e^{2\epsilon\gamma_E} \cdot 4^{-2\epsilon} \cdot \Gamma(-6+4\epsilon) \cdot \Gamma(2-\epsilon) \cdot \omega^{6-4\epsilon} e^{4i\pi\epsilon} \\
&\times \left[\Gamma(2-\epsilon) \cdot T^1_{\mu\rho\nu\sigma} + \Gamma(3-\epsilon) \cdot T^2_{\mu\rho\nu\sigma} \right], \qquad (3.3) \\
C^{\mathrm{X}}_{\bar{q}q}(\omega) = &- \frac{\alpha_s}{\pi} \cdot C_F \cdot \mathrm{Tr}[\Gamma_1 P_+ \Gamma_2] \cdot \mu^{2\epsilon} e^{\epsilon\gamma_E} \cdot 4^{-\epsilon} \cdot \Gamma(-3+2\epsilon) \cdot \omega^{3-2\epsilon} e^{2i\pi\epsilon} \\
&\times \left[\Gamma(2-\epsilon) \cdot T^1_{\mu\rho\nu\sigma} + \Gamma(3-\epsilon) \cdot T^2_{\mu\rho\nu\sigma} \right], \qquad (3.4)
\end{aligned}
$$

with

$$
\begin{aligned}
T^1_{\mu\rho\nu\sigma} &:= g_{\mu\rho} g_{\nu\sigma} - g_{\mu\sigma} g_{\nu\rho}\,, \qquad (3.5) \\
T^2_{\mu\rho\nu\sigma} &:= -\, g_{\nu\sigma} v_\mu v_\rho + g_{\mu\sigma} v_\nu v_\rho + g_{\nu\rho} v_\mu v_\sigma - g_{\mu\rho} v_\nu v_\sigma\,. \qquad (3.6)
\end{aligned}
$$

Notice that the tensor structures of $T^{1,2}_{\mu\rho\nu\sigma}$ all considered Wilson coefficients satisfy the symmetries imposed by the field strength tensors $G_{\mu\nu}$ and $G_{\rho\sigma}$. In particular, the expressions are anti-symmetric under the exchange of $\{\mu \leftrightarrow \nu\}$, $\{\rho \leftrightarrow \sigma\}$ and symmetric under the combined exchanges $\{\mu \leftrightarrow \rho, \nu \leftrightarrow \sigma\}$ and $\{\mu \leftrightarrow \nu, \rho \leftrightarrow \sigma\}$. The Wilson coefficient for the gluon condensate and higher mass dimension correction for the quark condensate share the same tensor structure as the coefficients stated in Eq. (3.3) and (3.4).

The Wilson coefficient of the gluon condensate, which corresponds to Fig. 2 (a) can be expressed as:

$$
C^{\mathrm{X}}_{G^2}(\omega) = \mathrm{Tr}[\Gamma_1 P_+ \Gamma_2 \not{v}] \cdot \frac{\mu^{2\epsilon} e^{\epsilon\gamma_E} \cdot 4^{-\epsilon}}{(4-2\epsilon)(3-2\epsilon)} \cdot \Gamma(-2+2\epsilon) \cdot \Gamma(2-\epsilon) \cdot \omega^{2-2\epsilon} e^{2i\pi\epsilon} \cdot T^1_{\mu\rho\nu\sigma}\,. \qquad (3.7)
$$

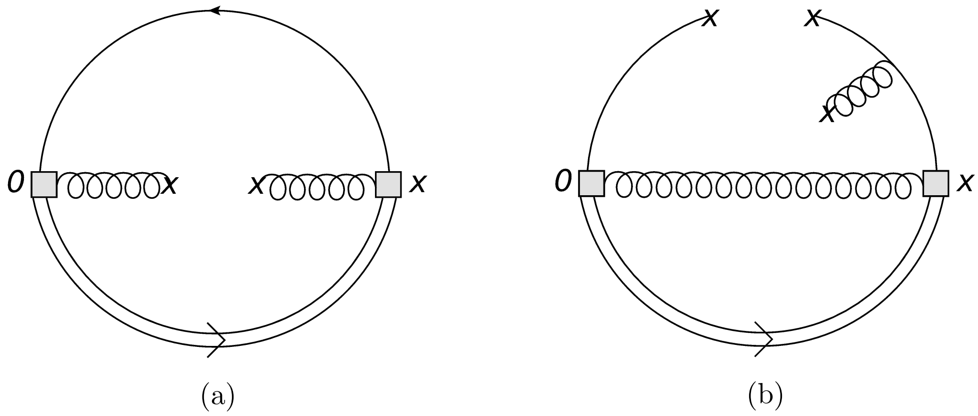

Figure 2: (a) shows the Feynman diagram for the dimension four contribution, (b) a schematic illustration of the dimension five condensate originating from the higher order expansion of the dimension three contribution in Figure 1.

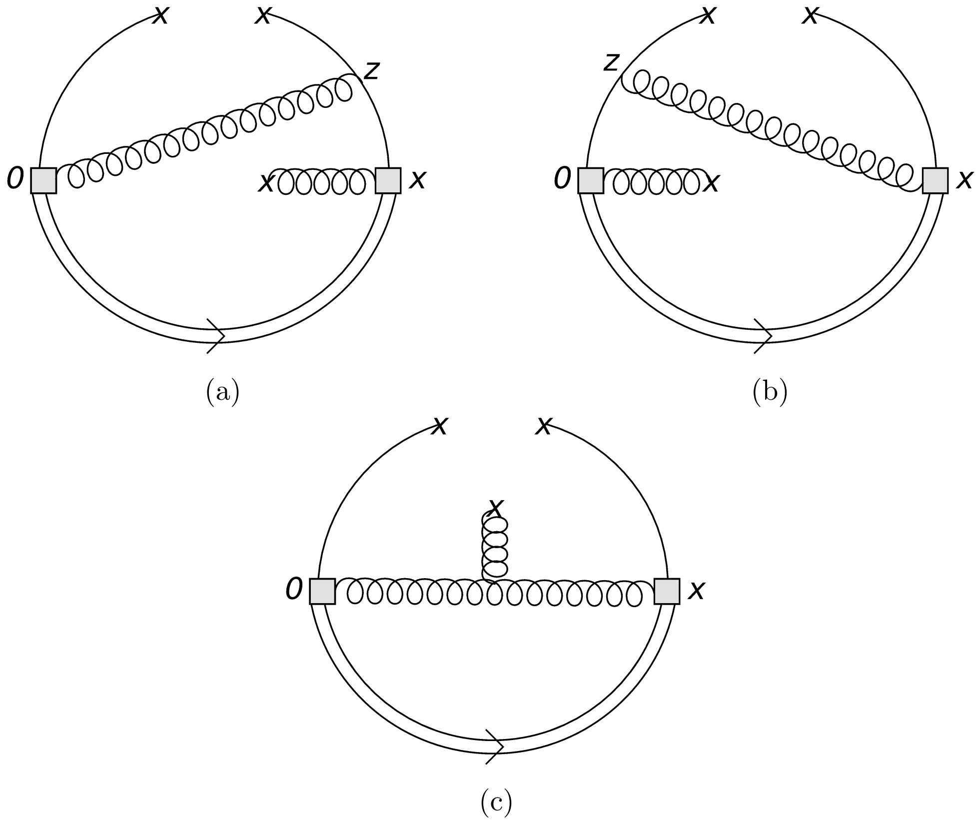

Figure 3: Feynman diagrams for dimension five condensate contributions.

The mass dimension five contributions are given as:

$$C^{\mathrm{X}}_{\bar{q}Gq,1}(\omega) = -\,\frac{\alpha_s}{\pi}\cdot C_F\cdot \mathrm{Tr}[\Gamma_1 P_+ \Gamma_2]\cdot \frac{\mu^{2\epsilon}e^{\epsilon\gamma_E}\cdot 4^{-\epsilon}}{(4-2\epsilon)}\cdot \Gamma(-3+2\epsilon)\cdot\Gamma(3-\epsilon)\cdot \omega^{1-2\epsilon}e^{2i\pi\epsilon}\cdot T^1_{\mu\rho\nu\sigma}\,, \tag{3.8}$$

$$C^{\mathrm{X}}_{\bar{q}Gq,2}(\omega) = \frac{\alpha_s}{4\pi} \cdot \frac{\mu^{2\epsilon} e^{\epsilon\gamma_E} \cdot 4^{-\epsilon}}{(4-2\epsilon)(3-2\epsilon)} \cdot \Gamma(-1+2\epsilon) \cdot \Gamma(1-\epsilon) \cdot \omega^{1-2\epsilon} e^{2i\pi\epsilon} \cdot \Big[\mathrm{Tr}[\Gamma_1 P_+ \Gamma_2 \sigma_{\mu\nu}\sigma_{\rho\sigma}] - (1-\epsilon) \cdot \mathrm{Tr}[\Gamma_1 P_+ \Gamma_2 \not{v} \mathrm{i}(v_\mu \gamma_\nu - v_\nu \gamma_\mu)\sigma_{\rho\sigma}]\Big] , \tag{3.9}$$

$$C^{\mathrm{X}}_{\bar{q}Gq,3}(\omega) = \frac{\alpha_s}{4\pi} \cdot \frac{\mu^{2\epsilon} e^{\epsilon\gamma_E} \cdot 4^{-\epsilon}}{(4-2\epsilon)(3-2\epsilon)} \cdot \Gamma(-1+2\epsilon) \cdot \Gamma(1-\epsilon) \cdot \omega^{1-2\epsilon} e^{2i\pi\epsilon} \cdot \Big[\mathrm{Tr}[\Gamma_1 P_+ \Gamma_2 \sigma_{\mu\nu}\sigma_{\rho\sigma}] + (1-\epsilon) \cdot \mathrm{Tr}[\Gamma_1 P_+ \Gamma_2 \sigma_{\mu\nu} \mathrm{i}(v_\rho \gamma_\sigma - v_\sigma \gamma_\rho)\not{v}]\Big] , \tag{3.10}$$

$$\begin{aligned} C^{\mathrm{X}}_{\bar{q}Gq,4}(\omega) = & -\frac{i\alpha_s}{192\pi} \cdot C_A C_F \cdot \mathrm{Tr}[\Gamma_1 P_+ \Gamma_2 \sigma_{\chi\beta}] \cdot \mu^{2\epsilon} e^{\epsilon\gamma_E} \cdot 4^{-\epsilon} \cdot \Gamma(-1+2\epsilon) \cdot \Gamma(2-\epsilon) \cdot \omega^{1-2\epsilon} e^{2i\pi\epsilon} \cdot \\ & \Big[(2-\epsilon)\cdot(-1+2\epsilon) \cdot \frac{\Gamma(\epsilon)}{\Gamma(-1+\epsilon)} \big(g_{\nu\chi} T^1_{\beta\sigma\mu\rho} + 2 \cdot g_{\beta\chi} T^1_{\mu\sigma\nu\rho} + 3 \cdot g_{\rho\chi} T^1_{\mu\sigma\beta\nu}\big) \\ & + g_{\mu\chi} T^3_{\nu\rho\beta\sigma} + g_{\nu\beta} T^3_{\mu\rho\sigma\chi} + 2 \cdot v^\beta v^\nu (g^{\mu\rho} g^{\sigma\chi} - g^{\mu\sigma} g^{\rho\chi}) + g_{\beta\chi} T^3_{\nu\sigma\mu\rho} + g_{\beta\chi} T^3_{\mu\rho\nu\sigma} - \mu \leftrightarrow \nu\Big] , \end{aligned} \tag{3.11}$$

with

$$T^3_{\nu\rho\beta\sigma} := g^{\mu\chi}\big(v^\nu v^\rho g^{\beta\sigma} - v^\nu v^\sigma g^{\beta\rho}\big) . \tag{3.12}$$

Nevertheless, the other contributions for the mass dimension five condensate (Fig. 3) possess a more complicated tensor structure, which still satisfies all symmetries described before. We obtain the total Wilson coefficient for the mass dimension five condensate if we sum up all four previous contributions, namely $C^{\mathrm{X}}_{\bar{q}Gq} = \sum_{k=1}^{4} C^{\mathrm{X}}_{\bar{q}Gq,k}$. The last two diagrams depicted in Fig. 4 are of mass dimension six and seven. Their

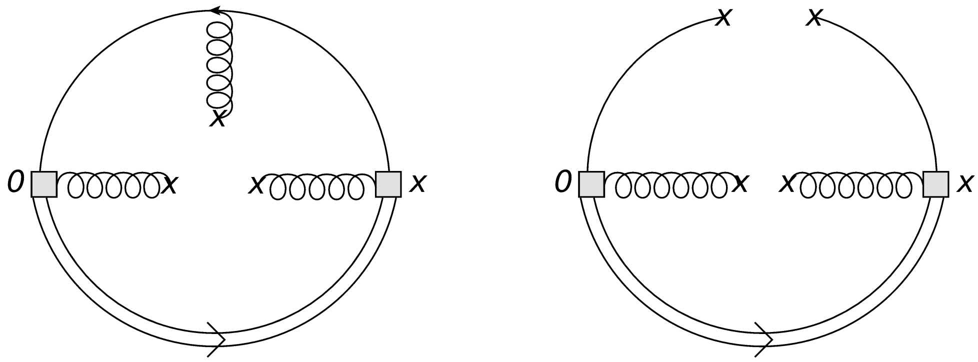

(a) (b)

Figure 4: Feynman diagrams for the dimension six and dimension seven condensate, which contribute to the leading order estimate of $\lambda^2_{E,H}$.

contributions are expected to be smaller compared to the dimension five contributions, such that we observe that the OPE starts to converge. Other contributions to mass dimension six are vanishing or are of $\mathcal{O}(\alpha_s^2)$. Thus, the triple-gluon condensate is the only relevant condensate at this order and the Wilson coefficient reads as:

$$C^{\mathrm{X}}_{G^3}(\omega) = \frac{\mu^{2\epsilon}e^{\epsilon\gamma_E}\cdot 4^{-\epsilon}}{64\pi^2}\cdot B_{\mu\lambda\rho\nu\sigma\alpha}\cdot\Gamma(2\epsilon)\cdot\Gamma(1-\epsilon)\cdot\omega^{-2\epsilon}e^{2i\pi\epsilon}\cdot\Big[\mathrm{Tr}[-i\cdot\Gamma_1 P_+\Gamma_2 \not{v}\sigma^{\lambda\alpha}]+ \mathrm{Tr}[\Gamma_1 P_+\Gamma_2(v^\alpha\gamma^\lambda - v^\lambda\gamma^\alpha)] + 2\cdot(1-\epsilon)\cdot\mathrm{Tr}[\Gamma_1 P_+\Gamma_2\not{v}v^\lambda v^\alpha]\Big] \tag{3.13}$$

where the expression $B_{\mu\lambda\rho\nu\sigma\alpha}$ is defined in Appendix A. Finally, we state the expression for the dimension seven contribution:

$$C^{\mathrm{X}}_{\bar{q}qG^2}(\omega) = -\,\mathrm{Tr}[\Gamma_1 P_+\Gamma_2]\cdot\frac{1}{\omega+i0^+}\cdot\frac{\pi^2}{2N_c(4-2\epsilon)(3-2\epsilon)}\cdot T^1_{\mu\rho\nu\sigma} \tag{3.14}$$

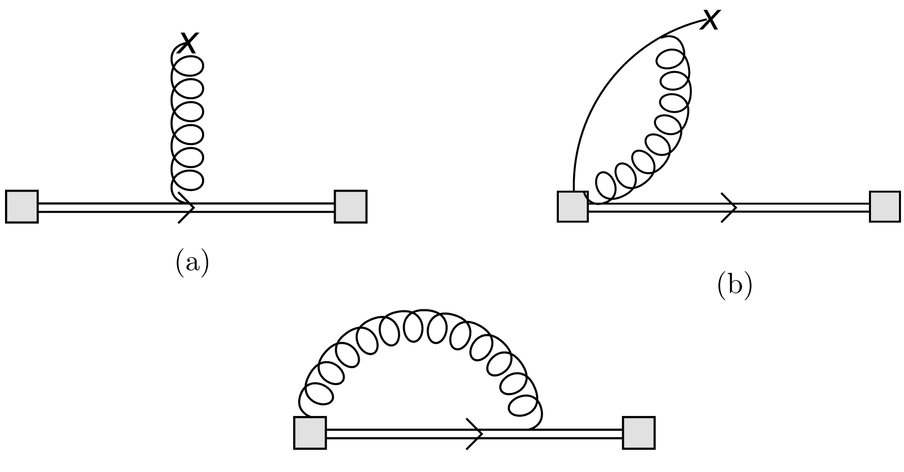

(c)

Figure 5: Vanishing subdiagrams in the Fock-Schwinger gauge.

According to Eq. (2.16) and (2.17), we still need to take the imaginary part of these diagrams. We choose to compute directly the loop diagrams and take the imaginary part of the resulting expression. Following Cutkosky rules, another approach would be to perform the calculation by considering all possible cuts for the diagrams. Apart from the diagrams in Figure 3, the diagrams are finite. (a) and (b) in Figure 3 include both a three-particle and a two-particle cut, where the latter requires a non-trivial renormalization procedure [47]. The optical theorem states that both calculations yield the same result.

Besides the diagram in Fig. 2 (b), all diagrams in Fig. 1-4 can generally be calculated by using perturbative methods. Figure 2 (b) stems from higher order corrections in the expansion of the non-perturbative quark condensate in Eq. (A.1). Moreover, the diagrams contributing to the quark-gluon condensate in Figure 3 (a) and (b) obey the same structure as the contributions in [19, 24] and hence a cross-check is possible after replacing the quark condensate by the quark-gluon condensate and keeping in mind that the Lorentz structures differ.

In our notation, α_s is defined to be $g_s^2/(4\pi)$ and C_F, C_A denote the two quadratic Casimir operators in a general SU(N) gauge group, satisfying

$$\begin{aligned} C_A &= N_c\,, \\ C_F &= \frac{N_c^2-1}{2N_c}\,, \end{aligned} \tag{3.15}$$

with N_c illustrating the number of colors. Depending on the conventions used during the computation, all results need to be multiplied by a factor of $4^{-\epsilon}$ (or $4^{-2\epsilon}$ in the perturbative case), which contributes to the finite part and does not change the imaginary part.

By taking the imaginary part of all Wilson coefficients discussed above and plugging the results into Eq. (2.23), (2.24) and performing the integration over ω up to the threshold parameter ω_{th}, we obtain the final expression for the sum rules:

$$\begin{aligned} F(\mu)^2\cdot(\lambda_H^2+\lambda_E^2)^2\,e^{-\bar\Lambda/M} = & \; \frac{\alpha_s N_c C_F}{\pi^3}\cdot 24M^7\cdot G_6\Big(\frac{\omega_{th}}{M}\Big) \\ & - \frac{\alpha_s C_F}{4\pi N_c}\cdot(C_A^2+6N_C)\cdot\langle\bar q g_s\sigma\cdot Gq\rangle\cdot M^2\cdot G_1\Big(\frac{\omega_{th}}{M}\Big) \\ & - \frac{\pi^2}{2N_c}\,\langle\bar q q\rangle\,\langle\frac{\alpha_s}{\pi}G^2\rangle\,, \end{aligned} \tag{3.16}$$

$$\begin{aligned} F(\mu)^2\cdot\lambda_H^4\,e^{-\bar\Lambda/M} = & \; \frac{\alpha_s N_c C_F}{\pi^3}\cdot 12M^7\cdot G_6\Big(\frac{\omega_{th}}{M}\Big) - \frac{\alpha_s C_F}{\pi}\,\langle\bar q q\rangle\cdot 6\cdot M^4\cdot G_3\Big(\frac{\omega_{th}}{M}\Big) \\ & + \frac{1}{2}\,\langle\frac{\alpha_s}{\pi}G^2\rangle\cdot M^3\cdot G_2\Big(\frac{\omega_{th}}{M}\Big) \\ & - \frac{\alpha_s C_F}{8\pi N_c}\cdot(C_A^2+6N_C)\cdot\langle\bar q g_s\sigma\cdot Gq\rangle\cdot M^2\cdot G_1\Big(\frac{\omega_{th}}{M}\Big) \\ & + \frac{\langle g_s^3 f^{abc}G^aG^bG^c\rangle}{64\pi^2}\cdot M\cdot G_0\Big(\frac{\omega_{th}}{M}\Big) - \frac{\pi^2}{4N_c}\,\langle\bar q q\rangle\,\langle\frac{\alpha_s}{\pi}G^2\rangle\,, \end{aligned} \tag{3.17}$$

$$\begin{aligned} F(\mu)^2\cdot\lambda_E^4\,e^{-\bar\Lambda/M} = & \; \frac{\alpha_s N_c C_F}{\pi^3}\cdot 12M^7\cdot G_6\Big(\frac{\omega_{th}}{M}\Big) + \frac{\alpha_s C_F}{\pi}\,\langle\bar q q\rangle\cdot 6\cdot M^4\cdot G_3\Big(\frac{\omega_{th}}{M}\Big) \\ & - \frac{1}{2}\,\langle\frac{\alpha_s}{\pi}G^2\rangle\cdot M^3\cdot G_2\Big(\frac{\omega_{th}}{M}\Big) - \frac{\alpha_s C_F}{2\pi}\cdot\langle\bar q g_s\sigma\cdot Gq\rangle\cdot M^2\cdot G_1\Big(\frac{\omega_{th}}{M}\Big) \\ & - \frac{\langle g_s^3 f^{abc}G^aG^bG^c\rangle}{64\pi^2}\cdot M\cdot G_0\Big(\frac{\omega_{th}}{M}\Big) - \frac{\pi^2}{4N_c}\,\langle\bar q q\rangle\,\langle\frac{\alpha_s}{\pi}G^2\rangle\,. \end{aligned} \tag{3.18}$$

For convenience, we introduced the function:

$$G_n(x) := 1-\sum_{i=0}^{n}\frac{x^i}{i!}e^{-x}. \tag{3.19}$$

We see that the sum rules for $\lambda_{H,E}^4$ in Eq. (3.17) and (3.18) have got the same expression for the perturbative contribution. This contribution is in addition to that positive, since we are studying a positive-definite correlation function in Eq. (2.6).

Furthermore, the quark, the gluon and the triple-gluon condensate in Eq. (3.17), (3.18) have different signs and the Wilson coefficients in Eq. (3.9), (3.10) and (3.11) vanish for λ_E^4. This will have implications on the stability of the sum rule for the parameter λ_E^4 and will be investigated in Section 4. The dimension three, four and six condensates do not appear in Eq. (3.16), since the sign differs in Eq. (3.18) compared to (3.17).

All sum rules involve the decay constant $F(\mu)$, whose calculation of the correlation function can be found, e.g. in Ref. [24]. We will just state the result including all $\mathcal{O}(\alpha_s)$ corrections without any renormalization group improvement. At this point the dimension six contribution coming from the expansion of the quark condensate is also introduced and the vacuum saturation approximation is used in the computation.

$$F^2(\mu) \cdot e^{-\bar{\Lambda}/M} = \frac{N_c M^3}{\pi^2} \int_0^{\omega_{th}/M} \mathrm{d}x \; x^2 e^{-x} \left(1 + \frac{3C_F\alpha_s}{2\pi}\left(\ln\left(\frac{\mu}{2Mx}\right) + \frac{17}{6} + \frac{2\pi^2}{9}\right)\right) - \\ \langle \bar{q}q \rangle \left(1 + \frac{3C_F\alpha_s}{2\pi}\right) + \frac{1}{16M^2} \langle \bar{q} g_s G \cdot \sigma q \rangle + \frac{\pi C_F \alpha_s}{72 N_c M^3} \langle \bar{q}q \rangle^2 \; . \quad (3.20)$$

4 Numerical Analysis

In this section we first compute the HQET parameters directly from the sum rules in Eq. (3.16) and (3.18) following the procedure described in Section 3. The numerical inputs for the necessary parameters ~~and constants~~ are given in Table 1. But when we investigate the optimal window for the Borel parameter M, we observe that the sum rules are dominated by higher resonances and the continuum contribution. This questions the reliability of our estimates for $\lambda^2_{E,H}(1\text{ GeV})$ and their ratio:

$$\mathcal{R}(\mu) = \frac{\lambda_E^2(\mu)}{\lambda_H^2(\mu)} \tag{4.1}$$

at $\mu = 1$ GeV. Hence, we consider combinations of Eq. (3.16), (3.17), (3.18) and (3.20).

Parameters	Value	Ref.
$\alpha_s(1\text{ GeV})$	0.471	[48]
$\langle\bar{q}q\rangle$	$(-0.242 \pm 0.015)^3$ GeV^3	[49]
$\langle\frac{\alpha_s}{\pi}G^2\rangle$	$(0.012 \pm 0.004)GeV^4$	[37]
$\langle\bar{q}gG\cdot\sigma q\rangle$ / $\langle\bar{q}q\rangle$	(0.8 $\pm$0.2) GeV^2	[50]
$\langle g_s^3 f^{abc}G^aG^bG^c\rangle$	(0.045 ± 0.01) GeV^6	[38]
$\bar{\Lambda}$	(0.55 ± 0.06) GeV	[51]

Table 1: List of the numerical inputs, which will be used in our analysis. The vacuum condensates are normalized at the point $\mu = 1$ GeV. For the strong coupling constant we use the two-loop expression with $\Lambda^{(4)}_{\text{QCD}} = 0.31$ GeV.

In Figure 6, the lower plot illustrates the sum rule $(\lambda_H^2 + \lambda_E^2)^2$ individually for each order in the power expansion of the sum rule in Eq. (3.16). Here, we see that the dimension three, four and six condensates do not contribute to the sum rule. The terms corresponding to the dimension five condensate provide the largest contribution and beyond this dimension the power expansion is expected to converge, which is indicated by the small contribution of mass dimension seven. The upper plot in Figure 6 shows the value of $(\lambda_H^2 + \lambda_E^2)^2$ as a function of M for different threshold parameter ω_{th}. This variation of the parameter ω_{th} indicates the stability of the sum rule, since the Borel parameter M and ω_{th} are correlated. Furthermore, it can be explicitly seen that in the highly non-perturbative regime with small M the condensate contributions become dominant and therefore the sum rule becomes unreliable. To find the optimal window of the threshold ω_{th}, we vary the function $F(\mu)$ in Eq. (3.20) for different values of ω_{th}, see Figure 9. As we can see, the decay constant $F(\mu)$ gives reliable values in the interval $0.8\,\text{GeV} \leq \omega_{th} \leq 1.0\,\text{GeV}$. In order to see whether our threshold choice gives reasonable results, we compute the physical decay constant f_B by using Eq. (2.3), see Figure 10. Another method to determine the interval for the threshold parameter ω_{th} is by taking the derivative with respect to the Borel parameter $\partial/\partial(-1/M)$ in Eq. (3.17) and (3.18). By dividing these expressions by the original sum rules in Eq. (3.17) and (3.18), we obtain an estimate for the parameter $\bar{\Lambda}$ that needs to be compatible with the value stated in Table 1. Both methods give the same interval for ω_{th}. We observe in Figure 10 that for $0.6\,\text{GeV} \leq M$ the curve becomes stable and converges for $\omega_{th} = 0.8$ GeV to the lattice QCD value. Although the error on the decay constant f_B given in Eq. (2.4) is small, we assume a conservative uncertainty of $15\% - 20\%$, because our sum rules only account for the leading contributions up to mass dimension seven. This yields the interval $0.8\,\text{GeV} \leq \omega_{th} \leq 1.0\,\text{GeV}$ for the threshold parameter ω_{th}.

Similarly, we plot higher dimensional contributions for λ_H^4 in the lower part of Figure 7, but in comparison to Figure 6 we observe that each power correction enhances the total value of λ_H^4. Again, the dimension five contribution leads to the largest contribution in Figure 7. The fact that correlation functions with a large mass dimension experience large contributions from local condensates with a high mass dimension for small values of the Borel parameter M is a well known fact and has been studied [22–24]. Nonetheless, as already observed in Eq. (3.16), contributions from dimensions greater than five become smaller indicating convergence of the OPE. The upper plot in Figure 7 shows again the sum of all leading contributions up to mass dimension seven for different threshold parameter ω_{th}. The determination of the threshold window for ω_{th} follows the same argumentation as for the sum rule in Eq. (3.16). In particular, both methods lead again to the same conclusion and we obtain the interval $0.8\,\text{GeV} \leq \omega_{th} \leq 1.0\,\text{GeV}$.

The sum rule for the parameter λ_E^4 in Eq. (3.18) requires further investigation. Figure 8 presents in the upper plot the sum of all leading contributions up to mass dimension seven, while in the lower plot each contributions is considered individually. In comparison to the sum rules in Eq. (3.16) and Eq. (3.17), the mass dimension three and four condensates contribute with the opposite sign to this sum rule. Since these contributions are large, this sum rule becomes unreliable and unstable compared to the previously studied sum rules. Additionally, the dominant dimension five contributions from Eq. (3.9), (3.10) and (3.11) do not appear in this sum rule, thus the extraction of an estimate for λ_E^2 from this sum rule gives an unreliable value. Nevertheless, the mass dimension six and seven contributions are smaller than the dimension five contributions, hence the OPE seems to converge. The fact that this sum rule becomes unstable can be seen from the threshold interval for ω_{th}. Only the argumentation via the decay constants $F(\mu)$ and f_B give an appropriate interval, namely 0.55 GeV $\leq \omega_{th} \leq 0.65$ GeV. Moreover, the variation of the threshold seems to be larger than for the sum rules in Eq. (3.16) and (3.17) indicating a less stable sum rule with larger uncertainties.

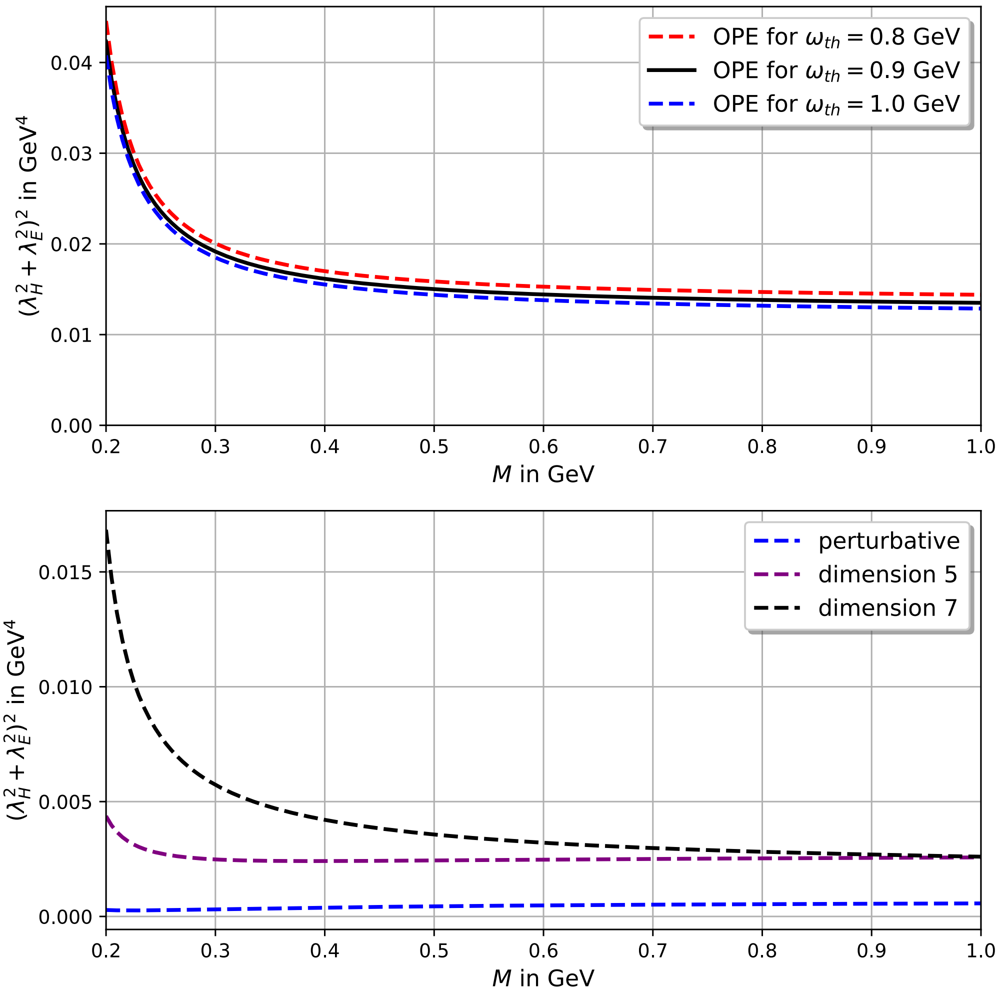

convergence?

Figure 6: The above figure shows the full OPE of Eq. (3.16) within the window $0.8\,\text{GeV} \leq \omega_{th} \leq 1.0\,\text{GeV}$. The lower figure shows the individual contribution of the OPE for $\omega_{th} = 0.9$ GeV. The plots are showing only the central values.

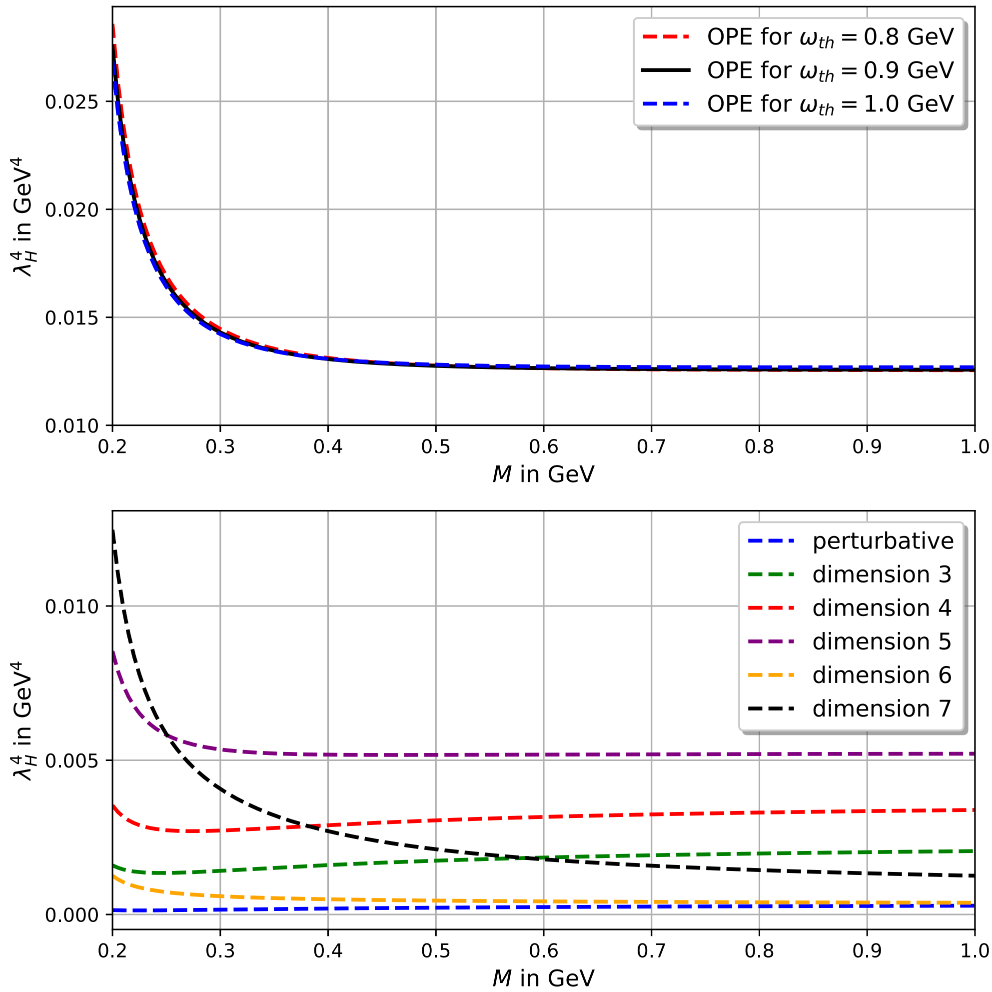

where is total?

Figure 7: The above figure shows the full OPE of Eq. (3.17) within the window $0.8\,\text{GeV} \leq \omega_{th} \leq 1.0\,\text{GeV}$. The lower figure shows the individual contribution of the OPE for $\omega_{th} = 0.9$ GeV. The plots are showing only the central values.

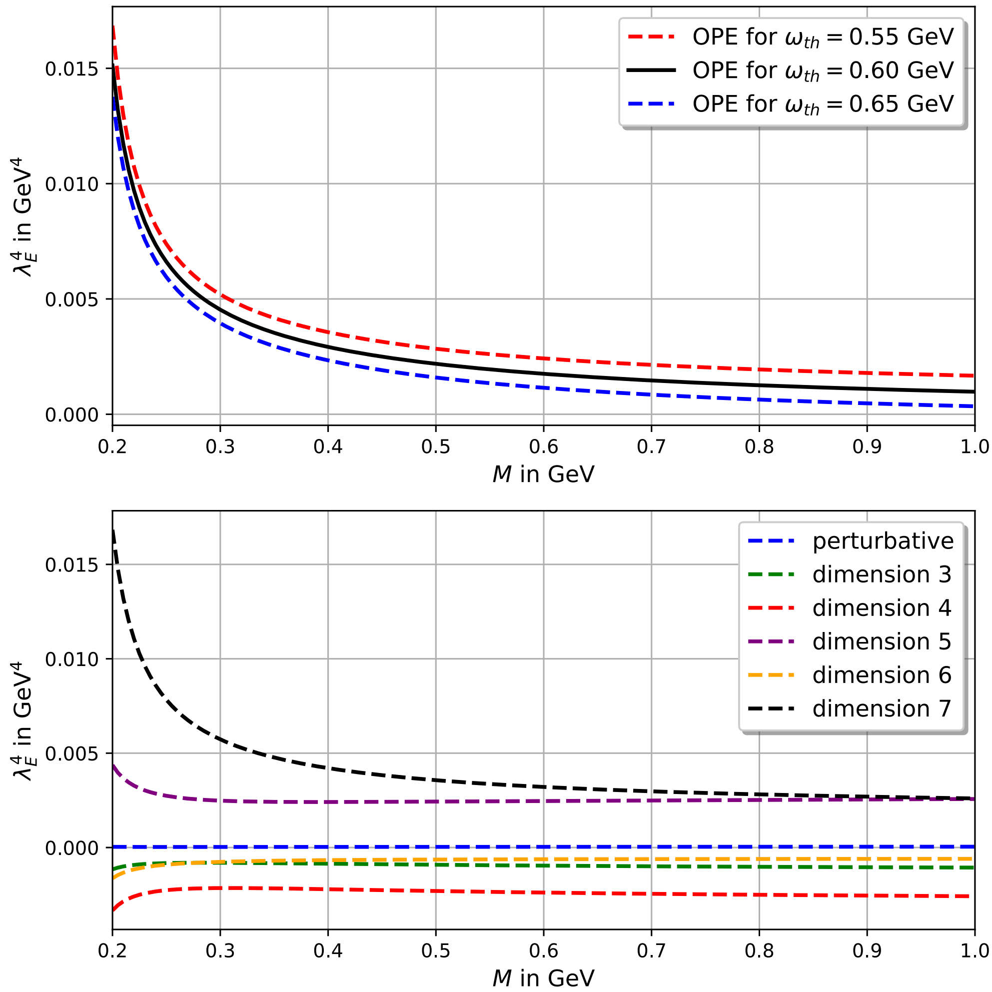

dim 7\sim dim 5

Figure 8: The above figure shows the full OPE of Eq. (3.18) within the window $0.55\,\text{GeV} \leq \omega_{th} \leq 0.65\,\text{GeV}$. The lower figure shows the individual contribution of the OPE for $\omega_{th} = 0.60$ GeV. The plots are showing only the central values.

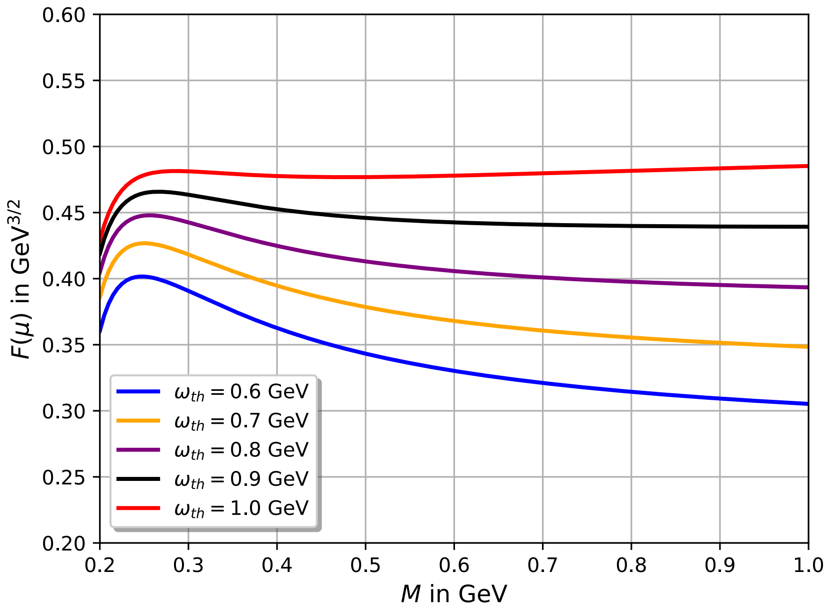

Figure 9: Comparison of the central values of the decay constant $F(\mu)$ for different values of ω_{th}. The value of the binding energy can be found in Table 1.

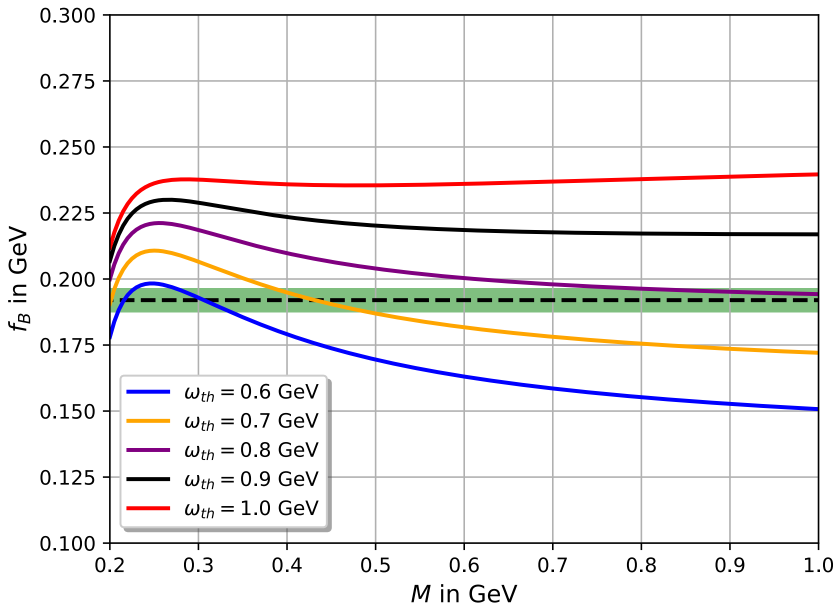

Figure 10: Comparison of the central values of the physical decay constant f_B with different values of ω_{th}. The dashed line indicates the lattice result and the shaded green area illustrates its corresponding uncertainty.

To obtain the lower bound for the Borel parameter M, we choose a value where the dimension seven condensate contribution is smaller than 40% of the total OPE. Notice that too small values of M spoil the convergence of the OPE since the condensate contributions become dominant. For the sum rules in Eq. (3.16) and (3.17), this condition is fulfilled for $0.5\,\text{GeV} \leq M$. Based on Fig. 6 and 7, we also see that for $0.5\,\text{GeV} \leq M$ the sum rule starts to become more reliable. As already mentioned, the sum rule for λ_E^4 in Eq. (3.18) is more unstable compared to λ_H^4 and $(\lambda_H^2 + \lambda_E^2)^2$ because of the decrease in the total sum due to mass dimension three, four and six contributions. As expected the method to obtain the lower bound of M does not work for λ_E^4. Instead, we choose the values based on Figure 8. We see that for $0.5\,\text{GeV} \leq M$ the OPE becomes more reliable and therefore a good choice for the lower bound. We are compensating the estimate of the lower bound in the uncertainty analysis.

For the determination of the upper bound of the Borel parameter we introduce:

$$R_{\text{cont.}} = 1 - \frac{\int_0^{\omega_{th}} \mathrm{d}\omega \frac{1}{\pi} \mathrm{Im}\Pi_X^{\text{OPE}}(\omega) e^{-\omega/M}}{\int_0^{\infty} \mathrm{d}\omega \frac{1}{\pi} \mathrm{Im}\Pi_X^{\text{OPE}}(\omega) e^{-\omega/M}} \qquad \text{for} \quad X \in \{H, E, HE\}\,. \tag{4.2}$$

The value of $R_{\text{cont.}}$ guarantees that the ground state still gives a sizeable contribution compared to the higher resonances and continuum contribution. Hence, for reliable results of the sum rule we expect $R_{\text{cont.}} \leq 50\%$ for $M \leq M_{\text{max}}$. Thus, Eq. (4.2) fixes the upper bound for the Borel parameter. But in the case of Eq. (3.16), (3.17) and (3.18), the continuum is dominant. Hence, an upper bound for M is not feasible according to this method.

To resolve this problem, we are considering two combinations of the sum rules in Section 3, which have the feature that $R_{\text{cont.}}$ becomes about 50% for a reasonable value of M. The combinations we will investigate are the following:

$$\frac{(\lambda_H^2 + \lambda_E^2)^2}{\lambda_H^4} = (1 + \mathcal{R})^2 \quad \text{and} \quad \frac{F(\mu)^2 + \lambda_H^4}{F(\mu)^2 - \lambda_E^4} \tag{4.3}$$

with $\mathcal{R}$ defined in Eq. (4.1). The combination $(1 + \mathcal{R})^2$ is a appropriate choice, because the dominant mass dimension five contributions due to Eq. (3.17) lower the value of $R_{\text{cont.}}$ significantly. On the other hand, the second combination in Eq. (4.3) is dominated by the large $\mathcal{O}(\alpha_s^0)$ and $\mathcal{O}(\alpha_s)$ contributions from $F(\mu)$ such that $\lambda_{E,H}^4$ become only small corrections. For both combinations in Eq. (4.3) the parameter is $R_{\text{cont.}} \leq 50\%$ for $M_{\text{max}} = 0.8$ GeV.

In Table 2 we summarize the lower and upper bounds for the parameters M and ω_{th}.

Sum rule	Borel window	threshold window
$(1+\mathcal{R})^2$	0.5 GeV $\leq M \leq$ 0.8 GeV	0.8 GeV $\leq \omega_{th} \leq$ 1.0 GeV
$(F(\mu)^2+\lambda_H^4)/(F(\mu)^2-\lambda_E^4)$	0.5 GeV $\leq M \leq$ 0.8 GeV	0.8 GeV $\leq \omega_{th} \leq$ 1.0 GeV

Table 2: Summary of the threshold and Borel window for the combination in Eq. (4.3).

In Figure 11 and 12 we plot both combinations as a function of M for different values of ω_{th} within its window.

Finally, we are at the point to extract $\mathcal{R}$ and $\lambda_{E,H}^2$ based on Eq. (4.3). The uncertainties of $\lambda_{E,H}^2$ and for the ratio $\mathcal{R}$ are partially determined by varying each input parameter individually according to their uncertainty, see Table 1. For the strong coupling constant we use the two-loop expression with $\Lambda_{\rm QCD}^{(4)} = 0.31$ GeV to obtain $\alpha_s(1\,\text{GeV}) = 0.471$. We vary $\Lambda_{\rm QCD}^{(4)}$ in the interval $0.29\,\text{GeV} \leq \Lambda_{\rm QCD}^{(4)} \leq 0.33\,\text{GeV}$, which corresponds to the running coupling $\alpha_s(1\,\text{GeV}) = 0.44 - 0.50$. In the last step, we square each uncertainty in quadrature:

$$
\begin{aligned}
\mathcal{R}(1\,\text{GeV}) = 0.1 &+ \begin{pmatrix}+0.03\\-0.03\end{pmatrix}_{\omega_{th}} + \begin{pmatrix}+0.01\\-0.02\end{pmatrix}_{M} + \begin{pmatrix}+0.01\\-0.01\end{pmatrix}_{\alpha_s} + \begin{pmatrix}+0.01\\-0.01\end{pmatrix}_{\langle\bar{q}q\rangle} \\
&+ \begin{pmatrix}+0.02\\-0.03\end{pmatrix}_{\langle\frac{\alpha_s}{\pi}G^2\rangle} + \begin{pmatrix}+0.05\\-0.04\end{pmatrix}_{\langle\bar{q}gG\cdot\sigma q\rangle} + \begin{pmatrix}+0.01\\-0.01\end{pmatrix}_{\langle g_s^3 f^{abc}G^aG^bG^c\rangle} \\
&= 0.1 \pm 0.07
\end{aligned}
\tag{4.4}
$$

$$
\begin{aligned}
\lambda_H^2(1\,\text{GeV}) = &\Bigg[0.12 + \begin{pmatrix}+0.002\\-0.003\end{pmatrix}_{\omega_{th}} + \begin{pmatrix}+0.002\\-0.004\end{pmatrix}_{M} \\
&+ \begin{pmatrix}+0.001\\-0.001\end{pmatrix}_{\langle\frac{\alpha_s}{\pi}G^2\rangle} + \begin{pmatrix}+0.001\\-0.001\end{pmatrix}_{\langle\bar{q}gG\cdot\sigma q\rangle}\Bigg]\,\text{GeV}^2 \\
&= (0.110 \pm 0.005)\,\text{GeV}^2
\end{aligned}
\tag{4.5}
$$

For λ_H^2, the variation of the strong coupling constant α_s, the dimension three and dimension six condensates do not change the central value significantly. Therefore, the uncertainty can be neglected.

$$
\begin{aligned}
\lambda_E^2(1\,\text{GeV}) = &\Bigg[0.01 + \begin{pmatrix}+0.003\\-0.004\end{pmatrix}_{\omega_{th}} + \begin{pmatrix}+0.002\\-0.001\end{pmatrix}_{M} + \begin{pmatrix}+0.001\\-0.001\end{pmatrix}_{\alpha_s} + \begin{pmatrix}+0.003\\-0.003\end{pmatrix}_{\langle\bar{q}q\rangle} \\
&+ \begin{pmatrix}+0.003\\-0.003\end{pmatrix}_{\langle\frac{\alpha_s}{\pi}G^2\rangle} + \begin{pmatrix}+0.005\\-0.004\end{pmatrix}_{\langle\bar{q}gG\cdot\sigma q\rangle} + \begin{pmatrix}+0.001\\-0.001\end{pmatrix}_{\langle g_s^3 f^{abc}G^aG^bG^c\rangle}\Bigg]\,\text{GeV}^2 \\
&= (0.01 \pm 0.008)\,\text{GeV}^2\,.
\end{aligned}
\tag{4.6}
$$

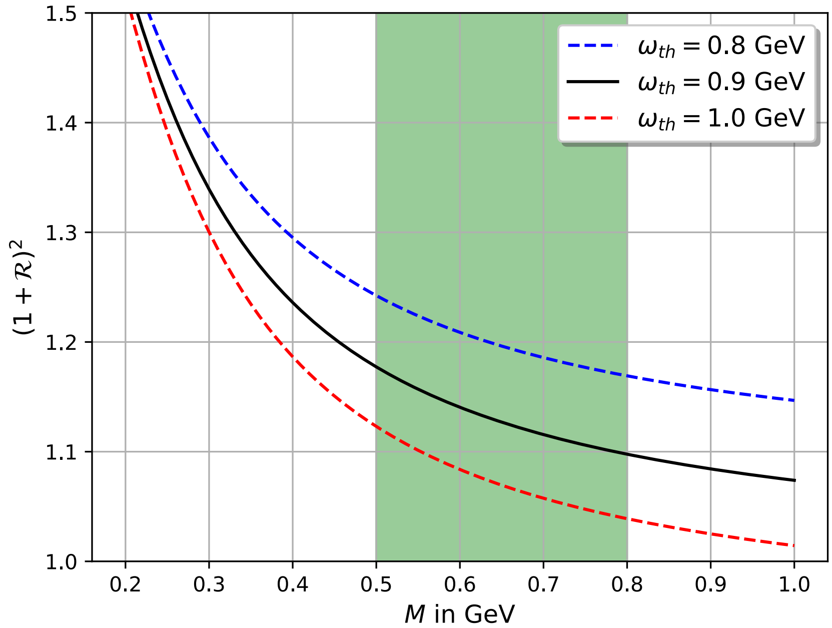

Figure 11: Borel sum rule for $(1+\mathcal{R})^2$ for the window $0.8\,\mathrm{GeV} \lesssim \omega_{th} \lesssim 1.0\,\mathrm{GeV}$.

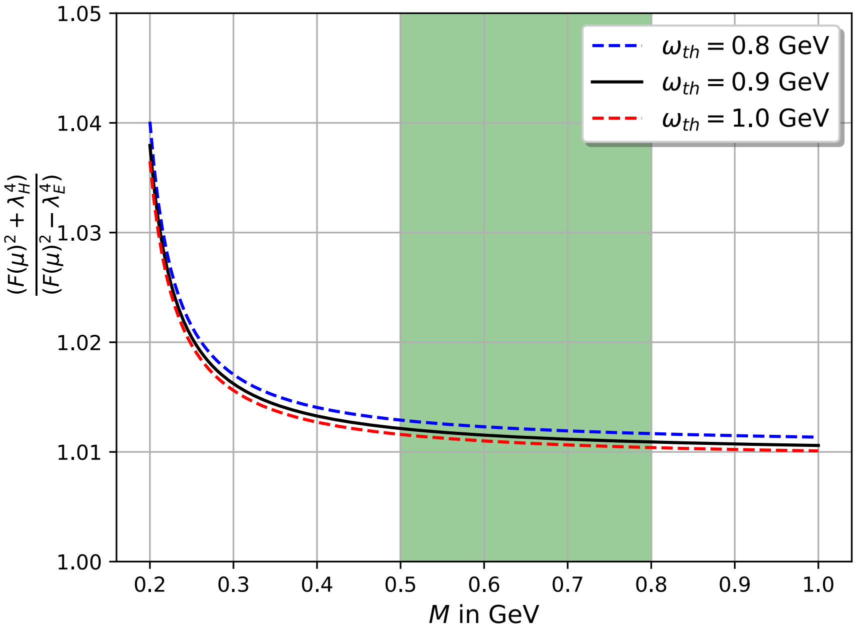

Figure 12: Borel sum rule for $(F^2(\mu)+\lambda_H^4)/(F^2(\mu)-\lambda_E^4)$ for the window $0.8\,\mathrm{GeV} \leq \omega_{th} \leq 1.0\,\mathrm{GeV}$.

Notice that the threshold parameter ω_{th} and the Borel parameter M are correlated, which can be deduced from the determination of the Borel window and the threshold interval. But since the variation of ω_{th} with respect to M is negligible, it is possible to choose one point in the parameter space of both parameters where the conditions from above are satisfied and obtain an estimate for the uncertainty by varying ω_{th}. Besides these contributions, there are other uncertainties due to several approximations and systematic errors. Since we truncated the perturbative series at $\mathcal{O}(\alpha_s)$ and the power corrections at dimension seven, we introduce another error which is more complicated to determine. Moreover, there is also an intrinsic uncertainty caused by the sum rule approach, for instance generated by the use of the quark-hadron duality. The total uncertainties stated in Eq. (4.4), (4.5) and (4.6) only list those quantities, which give deviations from the central values. A conservative estimate of the uncertainties leads to the following final results:

$$\lambda_E^2(1\text{ GeV}) = (0.01 \pm 0.01)\text{ GeV}^2 \tag{4.7}$$

$$\lambda_H^2(1\text{ GeV}) = (0.11 \pm 0.01)\text{ GeV}^2 \tag{4.8}$$

$$\mathcal{R} = 0.1 \pm 0.1. \tag{4.9}$$

If we consider instead directly Eq. (3.16), (3.17) and (3.18) and take the Borel window and the threshold parameter ω_{th} as shown in Table 2, we obtain the values:

$$\lambda_E^2(1\text{ GeV}) = (0.03 \pm 0.02)\text{ GeV}^2 \tag{4.10}$$

$$\lambda_H^2(1\text{ GeV}) = (0.11 \pm 0.02)\text{ GeV}^2 \tag{4.11}$$

$$\mathcal{R} = 0.3 \pm 0.2. \tag{4.12}$$

Although the sum rules in Eq. (3.16) to (3.18) are dominated by continuum contributions and higher resonances for the Borel window given in Table 2, we see that the set of parameters and their ratio $\mathcal{R}$ in Eq. (4.10) to (4.12) reproduce the values for $\lambda_{E,H}^2$ and $\mathcal{R}$ in Eq. (4.7) to (4.9) within the errors. In particular the estimate for λ_H^2 does not change, which indicates that the continuum contributions are well approximated by the sum rules in Eq. (3.17).

Our result for λ_E^2 in Eq. (4.7) is in full agreement with the result in [24]. Additionally, our result for λ_H^2 tends towards the result in [24]. The estimate for the $\mathcal{R}$-ratio is also in agreement with [52], but the central value differs considerable due to the small value of λ_E^2. A short comment is necessary at this point in order to discuss the deviations from the original estimates in [19]: One important difference in our analysis is that we included the $\mathcal{O}(\alpha_s)$ corrections for the HQET coupling constant $F(\mu)$, see Eq. (3.20). These contributions are known to be huge and question the convergence of the perturbative expansion in general [25]. First with the help of some simplified models [53] and later by explicit calculation of the order α_s^2 corrections it has been shown [26] that the perturbative series becomes convergent. Nevertheless, these sizeable contributions combined with $\mathcal{O}(\alpha_s)$ corrections of the dimension five condensate, the dimension six condensate and RGE improvement lead to the values of [24], which deviate from the first estimate of [19] by a factor of three and are in good agreement with our values. Consequently, the inclusion of $\mathrm{O}(\alpha_s)$ contributions into the sum rule is necessary for a good convergence of the OPE.

5 Conclusion

QCD

In this work we suggested alternative diagonal sum rules in order to derive estimates for the HQET parameters $\lambda_{E,H}^2$ and their ratio $\mathcal{R} = \lambda_E^2/\lambda_H^2$. We included all leading contributions to the diagonal three-particle quark-antiquark-gluon correlation function up to mass dimension seven ~~as parameterizations of the non-perturbative nature of the QCD vacuum~~. The advantage of these sum rules is that they are positive definite and we expect that the quark-hadron duality is more accurate compared to the previously studied correlation functions in [19, 24]. But we observe dominant contributions from the continuum and higher resonances due to the large mass dimension of the correlation function within these sum rules. This is why we consider combinations of these sum rules derived in Section 3 which satisfy the condition that the ground state contribution still gives a sizeable effect. Moreover, the OPE is expected to converge, because the investigated contributions beyond mass dimension five become smaller. We also include $\mathcal{O}(\alpha_s)$ corrections for the HQET decay constant $F(\mu)$, since these effects are known to be sizeable ~~huge~~ and indicate one reason for the deviation of the parameters $\lambda_{E,H}^2$ in the works by [19] and [24]. The values obtained in [19] and [24] compared to our result are listed in Table 3.

of ...currents

Parameters	Ref. [19]	Ref. [24]	Ref. [52]	this work
$\mathcal{R}(1\ \text{GeV})$	(0.6 ± 0.4)	(0.5 ± 0.4)	$0.4^{+0.5}_{-0.3}$	(0.1 ± 0.1)
$\lambda_H^2(1\ \text{GeV})$	$(0.18 \pm 0.07)\ \text{GeV}^2$	$(0.06 \pm 0.03)\ \text{GeV}^2$	–	$(0.11 \pm 0.01)\ \text{GeV}^2$
$\lambda_E^2(1\ \text{GeV})$	$(0.11 \pm 0.06)\ \text{GeV}^2$	$(0.03 \pm 0.02)\ \text{GeV}^2$	–	$(0.01 \pm 0.01)\ \text{GeV}^2$

correlation ?
?

Table 3: Comparison of our results for the parameters $\lambda_{E,H}^2$ and $\mathcal{R}$.
(to include only calculations, in fact [52] is an average of 19 and 24)

We see that our results are in good agreement with [24], while there are deviations between [19] and our result. With these new sum rules we obtain independent estimates for the parameters $\lambda_{E,H}^2$ and the $\mathcal{R}$-ratio, which are important ingredients for the second moments of the B-meson light-cone distribution amplitudes in B-meson factorization theorems. ??

can the missed alpha_s^2 corrections be estimates and included in uncertainty?

Acknowledgments

We would like to thank Alexander Khodjamirian for proposing this project to us, for his constant feedback throughout the work and for reading the manuscript ~~carefully~~. We thank Thomas Mannel for useful discussion and reading the manuscript. Additionally, we are grateful to Thorsten Feldmann and Alexei Pivovarov for helpful discussions. This work was funded by SFB XXX.

A Parametrization of the QCD Condensates

Here we present the condensates that we have used in the work. All results are based on [54] if not stated otherwise. First, we Taylor expand the following matrix element:

$$\begin{aligned} \langle 0|\, \bar{q}(0)\Gamma_1 P_+ \Gamma_2\, q(x)\, |0\rangle = {} & \langle 0|\, \bar{q}(0)\Gamma_1 P_+ \Gamma_2 q(0)\, |0\rangle + x^\mu \langle 0|\, \bar{q}(0)\Gamma_1 P_+ \Gamma_2 D_\mu q(0)\, |0\rangle \\ & + \frac{1}{2} x^\mu x^\nu \langle 0|\, \bar{q}(0)\Gamma_1 P_+ \Gamma_2 D_\mu D_\nu q(0)\, |0\rangle + \cdots \end{aligned} \tag{A.1}$$

The first term in Eq.(A.1) corresponds to the quark condensate.

$$\langle 0|\, \bar{q}^i_\alpha(0)\Gamma_{1,\alpha\beta} P_{+,\beta\gamma} \Gamma_{2,\gamma\delta}\, q^j_\delta(0)\, |0\rangle = \frac{1}{4N_c} \cdot \mathrm{Tr}[\Gamma_1 P_+ \Gamma_2]\, \langle \bar{q}q\rangle\, \delta^{ij}, \tag{A.2}$$

where (i,j) are color indices and $(\alpha,\beta,\gamma,\delta)$ are spinor indices. The second term in Eq.(A.1) does not contribute. Making use of the Dirac equation, we can rewrite the covariant derivative as:

$$\not{D} q = -i m_q q. \tag{A.3}$$

In HQET we assume $m_q = 0$ for light quarks.

Before we consider the third term in more detail, we parametrize the dimension five matrix element:

$$\langle 0|\, \bar{q}^i_\alpha(0) g_s G_{\mu\nu}(0) q^j_\delta(0)\, |0\rangle = \langle 0|\, \bar{q} g_s \sigma \cdot G q\, |0\rangle \cdot \frac{1}{4N_c d(d-1)} \cdot \delta^{ij} \cdot (\sigma_{\mu\nu})_{\delta\alpha} \tag{A.4}$$

The third term in Eq.(A.1) corresponds to the quark-gluon condensate.

$$\frac{1}{2} x^\mu x^\nu \cdot \langle 0|\, \bar{q}^i_\alpha(0) D_\mu D_\nu q^j_\delta(0)\, |0\rangle = \frac{x^2}{16 N_c d}\, \delta^{ij} \delta_{\alpha\delta} \cdot \langle 0|\, \bar{q} g_s \sigma \cdot G q\, |0\rangle \tag{A.5}$$

The gluon condensate can be parametrized as:

$$\langle 0|\, G^a_{\mu\nu} G^b_{\rho\sigma}\, |0\rangle = \frac{1}{d(d-1)(N_c^2-1)} \langle G^2\rangle\, (g_{\mu\rho} g_{\nu\sigma} - g_{\mu\sigma} g_{\nu\rho}) \tag{A.6}$$

Next is the parametrization of the triple-gluon condensate, which was denoted as $B_{\mu\lambda\rho\nu\sigma\alpha}$ in Eq. (3.13). The decomposition of the triple-gluon condensate has been investigated in [55]:

$$\langle g_s^3 f^{abc} G^a_{\mu\nu} G^b_{\rho\sigma} G^c_{\alpha\lambda}\rangle = \frac{\langle g_s^3 f^{abc} G^a G^b G^c\rangle}{d(d-1)(d-2)} \cdot \Big(g_{\mu\lambda} g_{\rho\nu} g_{\sigma\alpha} + g_{\mu\sigma} g_{\rho\alpha} g_{\lambda\nu} + g_{\rho\lambda} g_{\mu\alpha} g_{\nu\sigma} + g_{\alpha\nu} g_{\mu\rho} g_{\sigma\lambda} - g_{\mu\sigma} g_{\rho\lambda} g_{\alpha\nu} - g_{\mu\lambda} g_{\rho\alpha} g_{\nu\sigma} - g_{\rho\nu} g_{\mu\alpha} g_{\sigma\lambda} - g_{\sigma\alpha} g_{\mu\rho} g_{\nu\lambda} \Big) \tag{A.7}$$

The expression in Eq. (A.7) corresponds to the tensor $B_{\mu\lambda\rho\nu\sigma\alpha}$ introduced in Eq. (3.13).

References

[1] M. Beneke, G. Buchalla, M. Neubert, and C.T. Sachrajda. Qcd factorization for exclusive non-leptonic -meson decays: general arguments and the case of heavy–light final states. *Nuclear Physics B*, 591(1-2):313–418, Dec 2000.

[2] M. Beneke, G. Buchalla, M. Neubert, and C. T. Sachrajda. Qcd factorization forbdecays: Strong phases andcpviolation in the heavy quark limit. *Physical Review Letters*, 83(10):1914–1917, Sep 1999.

[3] M. Beneke and Th. Feldmann. Factorization of heavy-to-light form factors in soft-collinear effective theory. *Nuclear Physics B*, 685(1-3):249–296, May 2004.

[4] Howard Georgi. An Effective Field Theory for Heavy Quarks at Low-energies. *Phys. Lett. B*, 240:447–450, 1990.

[5] V. M. Braun, D. Yu. Ivanov, and G. P. Korchemsky. B-meson distribution amplitude in qcd. *Phys. Rev. D*, 69:034014, Feb 2004.

[6] Hiroyuki Kawamura, Jiro Kodaira, Cong-Feng Qiao, and Kazuhiro Tanaka. B-meson light cone distribution amplitudes in the heavy quark limit. *Phys. Lett. B*, 523:111, 2001. [Erratum: Phys.Lett.B 536, 344–344 (2002)].

[7] Bjorn O. Lange and Matthias Neubert. Renormalization group evolution of the B meson light cone distribution amplitude. *Phys. Rev. Lett.*, 91:102001, 2003.

[8] Guido Bell, Thorsten Feldmann, Yu-Ming Wang, and Matthew W Y Yip. Light-Cone Distribution Amplitudes for Heavy-Quark Hadrons. *JHEP*, 11:191, 2013.

[9] V. M. Braun, Yao Ji, and A. N. Manashov. Scale-dependence of the b-meson lcda beyond leading order from conformal symmetry, 2019.

[10] V.M. Braun, Yao Ji, and A.N. Manashov. Two-loop evolution equation for the B-meson distribution amplitude. *Phys. Rev. D*, 100(1):014023, 2019.

[11] Anne Mareike Galda and Matthias Neubert. Evolution of the b meson light-cone distribution amplitude in laplace space. *Phys. Rev. D*, 102:071501, Oct 2020.

[12] V.M. Braun, Yao Ji, and A.N. Manashov. Higher-twist B-meson Distribution Amplitudes in HQET. *JHEP*, 05:022, 2017.

[13] M. Beneke and J. Rohrwild. B meson distribution amplitude from B –> \gamma l \nu. *Eur. Phys. J. C*, 71:1818, 2011.

[14] M. Beneke, V. M. Braun, Yao Ji, and Yan-Bing Wei. Radiative leptonic decay b with subleading power corrections. *Journal of High Energy Physics*, 2018(7):154, July 2018.

[15] M. Beneke, V. Braun, Yao Ji, and Yan-Bing Wei. Radiative leptonic decay b with subleading power corrections. *Journal of High Energy Physics*, 2018, 07 2018.

[16] Yue-Long Shen, Zhi-Tian Zou, and Yan-Bing Wei. Subleading power corrections to the $b \to \gamma l \nu$ decay in the perturbative qcd approach. *Phys. Rev. D*, 99:016004, Jan 2019.

[17] V.M. Braun and A. Khodjamirian. Soft contribution to ¡mml:math altimg="si1.gif" overflow="scroll" xmlns:xocs="http://www.elsevier.com/xml/xocs/dtd" xmlns:xs="http://www.w3.org/2001/xmlschema" xmlns:xsi="http://www.w3.org/2001/xmlschema-instance" xmlns="http://www.elsevier.com/xml/ja/dtd" xmlns:ja="http://www.elsevier.com/xml/ja/dtd" xmlns:mml="http://www.w3.org/1998/math/mathml" xmlns:tb="http://www.elsevier.com/xml/common/table/dtd" xmlns:sb="http://www.elsevier.com/xml/common/struct-bib/dtd" xmlns:ce="http://www.elsevier.com/xml/common/dtd" xmlns:xlink="http://www.w3.org/1999/xlink" xmlns:cals="http://www.elsevier.com/xml/common/cals/dtd"¿¡mml:mi¿b¡/mml:mi¿¡mml:mo¿¡/mml:r and the b-meson distribution amplitude. *Physics Letters B*, 718(3):1014–1019, Jan 2013.

[18] Alexander Khodjamirian, Rusa Mandal, and Thomas Mannel. Inverse moment of the B_s-meson distribution amplitude from QCD sum rule. *JHEP*, 10:043, 2020.

[19] A. G. Grozin and M. Neubert. Asymptotics of heavy-meson form factors. *Physical Review D*, 55(1):272–290, Jan 1997.

[20] E.V. Shuryak. The structure of hadrons containing a heavy quark. *Physics Letters B*, 93(1):134 – 136, 1980.

[21] Patricia Ball, Vladimir M Braun, and Alexander Lenz. Higher-twist distribution amplitudes of the k meson in QCD. *Journal of High Energy Physics*, 2006(05):004–004, may 2006.

[22] Vladimir M. Braun and I.E. Filyanov. Conformal Invariance and Pion Wave Functions of Nonleading Twist. *Sov. J. Nucl. Phys.*, 52:126–134, 1990.

[23] Patricia Ball, Vladimir M. Braun, Y. Koike, and K. Tanaka. Higher twist distribution amplitudes of vector mesons in QCD: Formalism and twist - three distributions. *Nucl. Phys. B*, 529:323–382, 1998.

[24] Tetsuo Nishikawa and Kazuhiro Tanaka. Qcd sum rules for quark-gluon three-body components in the b meson, 2011.

[25] D.J. Broadhurst and A.G. Grozin. Operator product expansion in static-quark effective field theory. large perturbative correction. *Physics Letters B*, 274(3):421 – 427, 1992.

[26] A. A. Penin and M. Steinhauser. Heavy-light meson decay constant from qcd sum rules in the three-loop approximation. *Physical Review D*, 65(5), Jan 2002.

[27] Matthias Neubert. Heavy-meson form factors from qcd sum rules. *Phys. Rev. D*, 45:2451–2466, Apr 1992.

[28] S. Aoki et al. Review of lattice results concerning low-energy particle physics. *Eur. Phys. J. C*, 77(2):112, 2017.

[29] Adam F. Falk, Matthias Neubert, and Michael Luke. The residual mass term in the heavy quark effective theory. *Nuclear Physics B*, 388(2):363 – 375, 1992.

[30] Matthias Neubert. Heavy-quark symmetry. *Physics Reports*, 245(5-6):259–395, Sep 1994.

[31] Pietro Colangelo and ALexander Khodjamirian. Qcd sum rules, a modern perspective. *At The Frontier of Particle Physics*, page 1495–1576, Apr 2001.

[32] E. C. Poggio, H. R. Quinn, and S. Weinberg. Smearing method in the quark model. *Phys. Rev. D*, 13:1958–1968, Apr 1976.

[33] Ralf Hofmann. Operator product expansion and quark–hadron duality: facts and riddles. *Progress in Particle and Nuclear Physics*, 52(2):299 – 376, 2004.

[34] Kenneth G. Wilson. Non-lagrangian models of current algebra. *Phys. Rev.*, 179:1499–1512, Mar 1969.

[35] V.A. Novikov, Mikhail A. Shifman, A.I. Vainshtein, and Valentin I. Zakharov. Calculations in External Fields in Quantum Chromodynamics. Technical Review. *Fortsch. Phys.*, 32:585, 1984.

[36] R. Thomas, T. Hilger, and B. Kämpfer. Four-quark condensates in nucleon qcd sum rules. *Nuclear Physics A*, 795(1-4):19–46, Nov 2007.

[37] Philipp Gubler and Daisuke Satow. Recent progress in qcd condensate evaluations and sum rules. *Progress in Particle and Nuclear Physics*, 106:1–67, May 2019.

[38] Mikhail A. Shifman, A.I. Vainshtein, and Valentin I. Zakharov. QCD and Resonance Physics. Theoretical Foundations. *Nucl. Phys. B*, 147:385–447, 1979.

[39] V. Fock. Proper time in classical and quantum mechanics. *Phys. Z. Sowjetunion*, 12:404–425, 1937.

[40] Julian Schwinger. On gauge invariance and vacuum polarization. *Phys. Rev.*, 82:664–679, Jun 1951.

[41] D. Binosi, J. Collins, C. Kaufhold, and L. Theussl. Jaxodraw: A graphical user interface for drawing feynman diagrams. version 2.0 release notes. *Computer Physics Communications*, 180(9):1709–1715, Sep 2009.

[42] R. Mertig, M. Böhm, and A. Denner. Feyn calc - computer-algebraic calculation of feynman amplitudes. *Computer Physics Communications*, 64(3):345 – 359, 1991.

[43] Vladyslav Shtabovenko, Rolf Mertig, and Frederik Orellana. New developments in feyncalc 9.0. *Computer Physics Communications*, 207:432–444, Oct 2016.

[44] Vladyslav Shtabovenko, Rolf Mertig, and Frederik Orellana. FeynCalc 9.3: New features and improvements. *Comput. Phys. Commun.*, 256:107478, 2020.

[45] R. N. Lee. Presenting litered: a tool for the loop integrals reduction, 2012.

[46] Roman N Lee. Litered 1.4: a powerful tool for reduction of multiloop integrals. *Journal of Physics: Conference Series*, 523:012059, Jun 2014.

[47] Andrey G. Grozin and Matthias Neubert. Hybrid renormalization of penguins and dimension-5 heavy-light operators. *Nuclear Physics B*, 495(1-2):81–98, Jun 1997.

[48] K. G. Chetyrkin, J. H. Kuehn, and M. Steinhauser. Rundec: a mathematica package for running and decoupling of the strong coupling and quark masses, 2000.

[49] Matthias Jamin. Flavor symmetry breaking of the quark condensate and chiral corrections to the Gell-Mann-Oakes-Renner relation. *Phys. Lett. B*, 538:71–76, 2002.

[50] V.M. Belyaev and B.L. Ioffe. Determination of Baryon and Baryonic Resonance Masses from QCD Sum Rules. 1. Nonstrange Baryons. *Sov. Phys. JETP*, 56:493–501, 1982.

[51] P. Gambino, A. Melis, and S. Simula. Extraction of heavy-quark-expansion parameters from unquenched lattice data on pseudoscalar and vector heavy-light meson masses. *Phys. Rev. D*, 96:014511, Jul 2017.

[52] Sébastien Descotes-Genon, Alexander Khodjamirian, and Javier Virto. Light-cone sum rules for $B \to K\pi$ form factors and applications to rare decays. *JHEP*, 12:083, 2019.

we do not calcualate R !!

[53] E. Bagan, Patricia Ball, V.M. Braun, and H.G. Dosch. Qcd sum rules in the effective heavy quark theory. *Physics Letters B*, 278(4):457 – 464, 1992.

[54] P. Pascual and R. Tarrach. *QCD: Renormalization for the Practitioner*, volume 194. 1984.

[55] S.N. Nikolaev and A.V. Radyushkin. Vacuum corrections to qcd charmonium sum rules: Basic formalism and o(g3) results. *Nuclear Physics B*, 213(2):285 – 304, 1983.